

**UNCLASSIFIED**

**AD NUMBER**

ADB203789

**NEW LIMITATION CHANGE**

**TO**

Approved for public release, distribution  
unlimited

**FROM**

Distribution authorized to DoD only;  
Specific Authority; Proprietary Info.; 12  
Sep 95. Other requests shall be referred  
to Commander, Army Medical Research and  
Materiel Command, Fort Detrick, MD  
21702-5012.

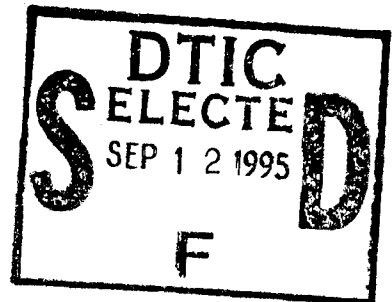
**AUTHORITY**

USAMRMC ltr dtd 21 Jan 2000

**THIS PAGE IS UNCLASSIFIED**

AD \_\_\_\_\_

CONTRACT NO: DAMD17-95-C-5044



TITLE: A Non-Invasive Deep Tissue PH Monitor

PRINCIPAL INVESTIGATOR(S): James E. Franke, Ph.D.

CONTRACTING ORGANIZATION: Rio Grande Medical Technologies, Inc.  
Albuquerque, New Mexico 87131

REPORT DATE: August 11, 1995

TYPE OF REPORT: Final - Phase I

PREPARED FOR: U.S. Army Medical Research and Materiel Command  
Fort Detrick, Maryland 21702-5012

**PROPRIETARY INFORMATION**

DISTRIBUTION STATEMENT: Distribution authorized to DOD Components only, Specific Authority. Other requests shall be referred to Commander, U.S. Army Medical Research and Materiel Command, Fort Detrick, Maryland 21702-5012

The views, opinions and/or findings contained in this report are those of the author(s) and should not be construed as an official Department of the Army position, policy or decision unless so designated by other documentation.

19950911 119

DTIC QUALITY INSPECTED 5

# REPORT DOCUMENTATION PAGE

**Form Approved  
OMB No. 0704-0188**

Public reporting burden for this collection of information is estimated to average 1 hour per response, including the time for reviewing instructions, searching existing data sources, gathering and maintaining the data needed, and completing and reviewing the collection of information. Send comments regarding this burden estimate or any other aspect of this collection of information, including suggestions for reducing this burden, to Washington Headquarters Services, Directorate for Information Operations and Reports, 1215 Jefferson Davis Highway, Suite 1204, Arlington, VA 22202-4302, and to the Office of Management and Budget, Paperwork Reduction Project (0704-0188), Washington, DC 20503.

1. AGENCY USE ONLY (Leave blank)			2. REPORT DATE: 11 Aug 1995	3. REPORT TYPE AND DATES COVERED Final, Phase I 15 Mar 95 - 14 Jul 95	
4. TITLE AND SUBTITLE  A Non-Invasive Deep Tissue PH Monitor			5. FUNDING NUMBERS DAMD17-95-C-5044		
6. AUTHOR(S)  James E. Franke, Ph.D.			8. PERFORMING ORGANIZATION REPORT NUMBER		
7. PERFORMING ORGANIZATION NAME(S) AND ADDRESS(ES)  Rio Grande Medical Technologies, Inc. Albuquerque, New Mexico 87131			10. SPONSORING/MONITORING AGENCY REPORT NUMBER		
9. SPONSORING/MONITORING AGENCY NAME(S) AND ADDRESS(ES)  U.S. Army Medical Research and Materiel Command Fort Detrick, Maryland 21702-5012			12a. DISTRIBUTION/AVAILABILITY STATEMENT  Distribution authorized to DOD Components only, Specific Authority. Other requests shall be referred to the Commander, U.S. Army Medical Research and Materiel Command, Fort Detrick, MD 21702-5012		
11. SUPPLEMENTARY NOTES			12b. DISTRIBUTION CODE		
13. ABSTRACT (Maximum 200 words)  The feasibility of pH determination in deep tissue, using non-invasive spectroscopic techniques, has been demonstrated for samples of both blood tissue phantoms and homogenized bovine muscle tissue phantoms. The tissue phantoms were designed to scatter light similarly to human tissue. Fourier transform near infrared reflectance spectra were obtained for the tissue phantom samples. The bovine samples varied in pH from 6.2 to 7.6, pH being adjusted using acid (lactic acid) or base (sodium hydroxide) additions. Commercial arterial blood gas (ABG) instrumentation was used as the pH reference. The reliability of the reference method and viability of the muscle homogenate was confirmed by nuclear magnetic resonance spectroscopy on a sample subset. Multivariate calibration of the VIS/NIR reflectance spectra against the ABG reference pH values yielded clinically relevant results. The standard error of prediction for pH was 0.049 pH units and 0.042 pH units using two spectral regions that were found to contain pH-specific information. The results demonstrate that it is feasible to make a deep tissue pH determination based on easily obtained visible/near infrared spectral data.			14. SUBJECT TERMS  Spectroscopy    Deep Tissue PH    Block Analyte		
15. NUMBER OF PAGES 37			16. PRICE ----		
17. SECURITY CLASSIFICATION OF REPORT  Unclassified	18. SECURITY CLASSIFICATION OF THIS PAGE  Unclassified	19. SECURITY CLASSIFICATION OF ABSTRACT  Unclassified	20. LIMITATION OF ABSTRACT  Limited		

## FOREWORD

Opinions, interpretations, conclusions and recommendations are those of the author and are not necessarily endorsed by the US Army.

Where copyrighted material is quoted, permission has been obtained to use such material.

Where material from documents designated for limited distribution is quoted, permission has been obtained to use the material.

JEF Citations of commercial organizations and trade names in this report do not constitute an official Department of Army endorsement or approval of the products or services of these organizations.

In conducting research using animals, the investigator(s) adhered to the "Guide for the Care and Use of Laboratory Animals," prepared by the Committee on Care and Use of Laboratory Animals of the Institute of Laboratory Resources, National Research Council (NIH Publication No. 86-23, Revised 1985).

For the protection of human subjects, the investigator(s) adhered to policies of applicable Federal Law 45 CFR 46.

In conducting research utilizing recombinant DNA technology, the investigator(s) adhered to current guidelines promulgated by the National Institutes of Health.

In the conduct of research utilizing recombinant DNA, the investigator(s) adhered to the NIH Guidelines for Research Involving Recombinant DNA Molecules.

In the conduct of research involving hazardous organisms, the investigator(s) adhered to the CDC-NIH Guide for Biosafety in Microbiological and Biomedical Laboratories.

 8/11/95  
PI - Signature Date

## TABLE OF CONTENTS

<b>1. INTRODUCTION.....</b>	<b>1</b>
1.1 BACKGROUND AND NATURE OF THE PROBLEM.....	1
1.2 PURPOSE AND SCOPE OF RESEARCH.....	1
<b>2. MAIN BODY.....</b>	<b>2</b>
2.1 DETERMINE OPTIMUM EXPERIMENTAL CONDITIONS (TASK 1) .....	2
2.2 CONSTRUCT A BLOOD LOOP (TASK 2) .....	3
2.3 DETERMINE pH IN BLOOD (TASK 3).....	4
2.3.1 <i>pH Determination of Intact Red Blood Cells using Flow Loop</i> .....	4
2.3.2 <i>pH Determination of Lysed Red Blood Cells using Flow Loop</i> .....	6
2.3.3 <i>pH Determination of Lysed Red Blood Cell Tissue Phantoms using Optical Cuvettes</i> .....	6
2.4 DEVELOP PROCEDURE FOR PREPARING MUSCLE CELL SUSPENSIONS (TASK 4).....	8
2.5 DETERMINE pH OF MUSCLE CELL SUSPENSIONS (TASK 5) .....	8
2.5.1 <i>pH Determination of Muscle Cell Tissue Phantoms</i> .....	8
2.5.2 <i>pH Determination of Muscle Cell Tissue Phantoms with NMR Validation</i> .....	9
<b>3. CONCLUSIONS.....</b>	<b>12</b>
<b>4. REFERENCES .....</b>	<b>13</b>

Accession For	
NTIS	CRA&I
DTIC	TAB
Unannounced	
Justification _____	
By _____	
Distribution / _____	
Availability Codes	
Dist	Avail and/or Special
E-4	

## 1. INTRODUCTION

### 1.1 BACKGROUND AND NATURE OF THE PROBLEM

An important measure of human health is a subject's acid-base status, since disturbances in acid-base regulation may have serious effects on metabolic activity, circulation, and the central nervous system. Currently, acid-base status is assessed using arterial blood gas (ABG) measurements, which require a blood draw and access to laboratory equipment not suitable for field use. Significant blood loss or shock resulting from trauma is often manifested in poor perfusion of peripheral tissue such as skeletal muscle. The consequence of an inadequate supply of blood to skeletal muscle is a local build-up of carbon dioxide and lactic acid, both of which lower pH in the skeletal muscle. Studies by Takano et al.<sup>1</sup> on animal models indicate that muscle pH (and muscle ppCO<sub>2</sub>) are more sensitive to decreased blood volume and to tissue ischemia than is arterial pH. Consequently, a non-invasive deep tissue pH monitor has enormous value as a mechanism for rapid and effective triage of wounded soldiers on the battlefield.

### 1.2 PURPOSE AND SCOPE OF RESEARCH

The overall purpose and scope of the research in Phase I was to demonstrate the feasibility of a deep tissue non-invasive pH monitor using visible/infrared spectroscopy and multivariate calibration techniques. In the proposed Phase I research, feasibility would be measured by the ability to quantify the pH of red blood and muscle cell samples based upon their visible and/or near infrared spectra. Reference pH values for these calibrations would be obtained using a commercially available blood gas analyzer, and careful experimental design techniques would be used to prepare the red blood and muscle cell samples. In Phase I research we also proposed to investigate the spectral characteristics and chemical species that are responsible for pH prediction. These steps would assure that true pH predictions are achieved, and improve our understanding of what physical effects are important to successful non-invasive deep tissue pH monitoring.

This last statement concerning the understanding of physical effects caused by pH changes deserves clarification. RGMT, Inc. possesses substantial expertise in chemometrics, which includes the subdisciplines of multivariate calibration and experimental design.<sup>2</sup> Chemometrics can be defined as the application of statistical and mathematical methods to the analysis of chemical data. Although it is possible with chemometrics simply to allow the computer to interpret the spectroscopic data, we seek first to identify and understand the source of spectroscopic data that are leading to the property prediction, in this case pH. Furthermore, we seek to carefully design our studies so that pH is made to vary orthogonally to spurious chemical or physical changes in the samples and to environmental or instrumental changes. These approaches maximize the likelihood of building a robust calibration model that correlates only to analyte-specific changes in the spectroscopic data.

The discussion to follow will illustrate that all of the specific tasks that were proposed for the Phase I research have been successfully completed. Non-invasive deep tissue pH measurement using chemometric analysis of spectral data is feasible. The Phase I results suggest that a small device, such as a multiple diode device perhaps as small as a quarter, could eventually be developed to provide the non-invasive pH measurement.

## 2. MAIN BODY

In our Phase I proposal, we identified the following specific tasks to be performed:

- TASK 1: Ascertain optimum experimental conditions for the measurement of pH in blood and tissue.
- TASK 2: Construct a "blood loop" for the determination of blood pH.
- TASK 3: Determine pH in blood. Produce and carry out a carefully designed experiment.
- TASK 4: Develop and test a procedure for preparing suspensions of muscle cells that can be tonometered to specified pH.
- TASK 5: Determine pH in suspensions of muscle cells.
- TASK 6: Prepare a Phase I report.

The discussion that follows will address each proposed task. We will describe the experimental methods used to accomplish each task, the results that were obtained, and the importance of the results to the goals of Phase I research. Based upon what was learned during the research phase, some of the tasks were modified from what was originally proposed. The rationale for these changes will be discussed in detail. In all cases, the changes added valuable, confirming evidence that helped demonstrate the feasibility of making non-invasive deep tissue pH measurements.

### 2.1 DETERMINE OPTIMUM EXPERIMENTAL CONDITIONS (TASK 1)

The overall goal in Task 1 was to determine the optimum experimental conditions for the determination of pH in blood and deep tissue. Specifically, we proposed to obtain visible (VIS) and/or near infrared (NIR) spectra using grating spectrographs equipped with a charge-coupled device (CCD) silicon array for the 500-900 nm region and a linear germanium (Ge) array for the 900-1800 nm region. We proposed using chemometrics to quantify pH from the measured spectra, and we anticipated the need to develop spectral preprocessing methods to minimize the effects of sample light scattering.

The determination of the pH of red blood cell samples was proposed as a starting point for Phase I research for the following reasons: (1) blood is present in and around deep tissue, so its spectroscopic signature must be recognized, (2) blood is known to scatter light, as does tissue, so the effects of scattering on pH prediction can be evaluated, (3) blood pH can be varied in a systematic way, and (4) standard electrochemical methods are available for measuring blood pH, which can then be used as the reference pH values for calibrating the VIS/NIR spectral data.

We performed several initial whole red blood cell studies to determine the optimal experimental conditions. Specifically, the method of sampling as well as the optimal instrumentation platform were carefully examined. For whole blood samples, we found that reflectance spectroscopy was sub-optimal due to the small amount of backscattered light available from the samples. To achieve better spectra of the whole blood samples, we used transmission spectroscopy. However, in tissue, which is a highly scattering medium<sup>3</sup>, we believe reflectance spectroscopy is the best optical sampling method. Our goal in initially measuring absorbance spectra of whole blood was to obtain spectral data of high enough quality to ascertain whether pH calibration was possible and to determine the physical basis for the calibration.

Based upon the observed scattering variations, we developed an improved scatter correction algorithm. Published methods for scatter correction calculate a global slope for correcting spectra. Our algorithm enhances this type of scatter correction by calculating a wavelength-dependent slope plus a global offset to scatter-correct the spectral data. The technique has worked well in removing gross baseline variations in the data, which typically reduce the complexity of our calibration models.

Additional whole blood studies also revealed that more light throughput would be advantageous at longer wavelengths, regardless of whether reflectance or transmittance spectra are measured, since blood and tissue strongly absorb light at these wavelengths due to their high water content. In situations of high sample absorbance, a Fourier transform instrument provides superior performance. Thus, we decided to use Fourier transform NIR (FT-NIR) spectrophotometers equipped with single-element photodetectors for recording the longer wavelength spectra. This instrument replaced the proposed grating spectrograph equipped with a linear Ge array detector. As we focused on optical throughput issues, we also investigated additional types of detectors that would be more sensitive at longer wavelengths, that is, above 1500 nm. Our investigation revealed that an indium antimonide (InSb) photodetector has superior sensitivity in the 1500-1800 nm range when compared to a germanium photodetector. The Ge detector is optimal for the 1000-1500 nm range, and a silicon (Si) photodetector is optimal for wavelengths below 1000 nm. Thus, we chose to collect FT-NIR spectra using all of these detectors to optimize our sensitivity over a wide spectral region (670-1800 nm). The Si photodetector was used to compare with the results from the CCD Si array (500-900 nm). The optimum pathlengths were 1 mm for the longer wavelengths (FT-NIR detectors) and 2 to 5 mm for the shorter wavelengths (CCD Si array).

Our initial whole blood studies, then, suggested that the best experimental conditions for determining whole blood pH would be to collect absorbance spectra using two instruments: an FT-NIR spectrophotometer equipped with three separate but simultaneously operating single-element photodetectors (670-1800 nm) and a spectrograph equipped with a CCD Si array (500-900 nm).

## 2.2 CONSTRUCT A "BLOOD LOOP" (TASK 2)

We proposed in Task 2 to build a blood flow loop that would contain two optical cells for measuring the VIS/NIR spectra of intact red blood cell samples. The rationale for using a flow loop was as follows: (1) to minimize beam heating of the sample by flowing the sample, (2) to minimize settling of the red blood cells that would introduce undesirable scattering changes and concentration gradients, (3) to allow the same sample to be measured with two different instruments, and (4) to reduce the amount of blood needed per sample.

During initial whole blood trials, we discovered that the flow loop must be built from stainless steel tubing. When perfluorinated polymer tubing was used to construct the loop, the partial pressure of oxygen (and sometimes of carbon dioxide) varied from the beginning to the end of the flow loop. Temperature sensors placed directly before and after the flow cells indicated only minor changes in sample temperature due to absorption of energy from the optical beam. About 6 cc of blood was required to flow the sample long enough to acquire two minutes of spectroscopic data. The final flow loop design is shown schematically in Figures 1a and 1b. The sample delivery subsystem (Figure 1a) allows the sample to be introduced at a constant rate

using an Infusion Pump. The heater blocks shown in Figure 1a maintain the sample temperature at 37°C. A three-way valve exists at the end of the flow loop so that the sample blood gas values can be checked to compare with pre-flow-loop values. The flow loop is then forward-washed with a detergent (Wash #1) and then backwashed with water, then methanol, and finally air to prepare it for the next sample. The environmental control subsystem (Figure 1b) was designed to maintain the air surrounding the flow loop and flow cells at 37°C.

The initial trials using the final design for the flow loop showed that blood cell settling could be minimized by increasing the flow rate, but not be completely eliminated. However, a too rapid flow rate caused blood cell channeling through the center of the optical flow cells, especially if pathlengths longer than about 2 mm were used. Channeling occurs when the blood flows more rapidly through the center of the optical flow cell than it does around the edges. Thus, the effects of cell settling and channeling were minimized by choosing the proper flow rate and optical flow cell pathlength for the red blood cell samples. Overall, the flow loop performed well, given the inherent difficulty of sampling intact red blood cells. Intact red blood cells are relatively large particles, having one dimension as large as 7  $\mu\text{m}$ . To put this size in perspective, Brownian motion can suspend particles in solution indefinitely only when the particles have a diameter of 0.1  $\mu\text{m}$  or less. Calculations show that a particle on the order of 10  $\mu\text{m}$  can settle out of solution at a rate of about 0.2 cm/min., which would introduce a substantial light scattering variation and concentration gradients during a two minute spectral data acquisition period. Hence, we believe the flow loop design in Figures 1a and 1b represents an optimized method for sampling intact red blood cells.

### 2.3 DETERMINE pH IN BLOOD (TASK 3)

As a starting point for Phase I research, we had proposed executing studies to determine the pH in whole blood (see Section 2.1), which would be obtained from donors. We proposed tonometering samples to desired pH levels while maintaining variations in the partial pressure of oxygen ( $\text{ppO}_2$ ) and the partial pressure of carbon dioxide ( $\text{ppCO}_2$ ) that were as orthogonal as possible to pH changes. In addition to tonometry, acid or base additions would be used to drive pH to the target values. The target pH values would be reached by using the Sigaard-Anderson "base excess" model<sup>4,5</sup> to calculate the proper gas values to tonometer and the proper acid or base amounts to add. We proposed using hydrochloric acid (or lactic acid) and sodium hydroxide as acid and base sources. We had further proposed collecting spectra over the 500-1800 nm region (2 minutes signal averaging per sample) and then calibrating the spectral data using pH reference values measured by a commercial blood gas analyzer.

#### 2.3.1 pH Determination of Intact Red Blood Cells using Flow Loop

Whole blood was obtained from donors, and a given calculated amount of acid or base was added to the blood using the Sigaard-Anderson model<sup>4,5</sup>. The samples were then tonometered for 10 minutes to equilibrate the  $\text{CO}_2$ ,  $\text{O}_2$ , and  $\text{N}_2$  gases to the desired gas levels. Following tonometry, we passed the intact whole red blood cell samples through the flow loop (Figures 1a and 1b). While the sample flowed through the loop, FT-NIR and VIS/NIR spectra of the intact whole red blood cell samples were obtained using the two instruments previously described (see Section 2.1). The flow loop possessed a 1 mm pathlength for the three FT-NIR detectors and a 2 mm pathlength for the CCD silicon detector.

Our experimental design (Figure 2) for the preparation of the samples shows the target pH and bicarbonate ion ( $\text{HCO}_3^-$ ) values that we sought to achieve using tonometry and acid/base addition. The target range for pH variation was 6.8-7.8 pH units. The solid curves in Figure 2 define reasonable physiological boundaries for  $\text{ppCO}_2$  in relation to pH and  $\text{HCO}_3^-$  levels. Outside these boundaries, life is not possible. The upper solid curve represents the 60 mmHg  $\text{ppCO}_2$  isobar, while the lower curve represents the 10 mmHg  $\text{ppCO}_2$  isobar. A Latin Hypercube experimental design with a D-optimality criterion was used, which provides orthogonal variation among the components and more evenly distributes the values over the range of variation. The goal is to orthogonalize component variations, but as Figure 2 shows, the physiological constraints of the bicarbonate buffer system in blood preclude a perfectly orthogonal design. It is important to recognize that other blood gas components (not shown in Figure 2) have also been made to vary orthogonally (or as nearly as possible) to both pH and  $\text{HCO}_3^-$ . The samples were also prepared in random order so that pH would not correlate with sample run order.

As an example of the pH calibration results that were obtained, we will discuss the FT-NIR absorbance spectra that were obtained using the InSb detector. These spectra are shown in Figure 3. The large band at  $7000 \text{ cm}^{-1}$  (1425 nm) and the edge of the highly absorbing band just below  $5500 \text{ cm}^{-1}$  (1820 nm) are overtone absorptions of water in blood. The spectra also exhibit relatively large baseline variations. These variations could be caused by differences in the light scattering properties of the whole blood samples and inhomogeneity of the flow of the blood through the optical flow cells. The results obtained by calibrating the absorbance spectra in Figure 3 against the reference pH values from the ABG analyzer yielded a cross-validated standard error of prediction (SEP) for pH in whole blood of 0.050 pH units. These results are shown graphically in Figure 4, which shows that pH was predicted well over the entire range of pH variation. Figure 4 also shows that pH values are well distributed over the range of pH so that the model for pH is more robust. The line through the points is the identity line, which means that if the predicted pH values exactly matched the reference pH values, then the points would all lie precisely on the identity line. The SEP is a metric that summarizes how well the points as a whole fall on the identify line. The equation for calculating the pH SEP for all results

$$\text{discussed in this report is } \text{SEP} = \sqrt{\frac{\sum_i (\text{reference} - \text{predicted})_i^2}{\text{number of samples}}}, \text{ summing over all samples.}$$

The results obtained for pH determination in whole blood using the flow loop and absorption spectroscopy were encouraging. We achieved pH prediction with a precision of 0.05 pH units, which is a clinically useful measure. However, careful examination of the spectroscopic data revealed that the observed spectral baseline changes correlated with pH prediction. We hypothesized that these large spectral changes were caused by cell size changes resulting from our experimental manipulation of the blood pH. This hypothesis was confirmed by additional experimentation and review of the literature<sup>6-8</sup>. We determined that our experimental protocol was introducing the observed spectral artifacts, which produced spuriously good results and possibly obscured the identification of a reliable spectroscopic source(s) of pH information. For these reasons, we modified our research proposal to include the study of pH variation in lysed red blood cells.

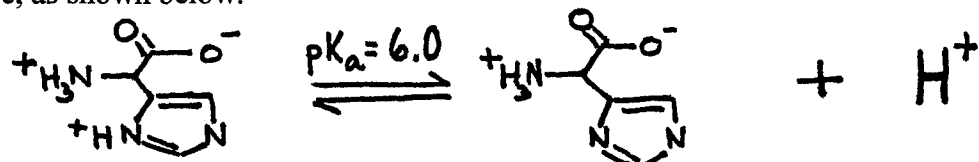
### 2.3.2 pH Determination of Lysed Red Blood Cells using Flow Loop

The effects of scattering from the whole blood samples, especially when one considers that the red blood cell changes its size and shape with pH<sup>6-8</sup>, makes it difficult to ascertain the subtle changes in the spectral data due to chemical effects caused by varying the sample pH. A sample with the same chemical make-up as whole blood, but without the cell walls, will produce spectral features that vary with pH identical to those in whole blood. Lysing whole blood to eliminate the red blood cell membranes produces samples that can be used to identify the spectral features, and the chemical species, that respond to pH changes.

Lysed blood was obtained by the following protocol: (1) sonicate fresh whole blood for 60 seconds to disrupt the cell membranes, (2) centrifuge the lysate for 10 minutes at 3000 rpm, and (3) collect the supernatant. The experimental design for varying the pH of the lysed blood samples was very similar to that used for the intact red blood cells (see Figure 2).

A total of 35 lysed blood samples were prepared and introduced to the flow loop/spectrometer system. The absorbance spectra obtained using the FT-NIR InSb detector are shown in Figure 5. The general appearance of these data are similar to those in Figure 2, e.g., the water bands have approximately the same absorbance values, but the baseline shifts that were caused by the light scattering from intact blood cells have been eliminated.

The calibration of the spectral data yielded an SEP of 0.03 pH units. These results are shown graphically in Figure 6. Elimination of the scattering effects made it much easier to identify the source of spectroscopic information specific for pH. The approach used to identify the important spectral features is to examine the loading vectors generated by the partial least squares (PLS) decomposition<sup>2</sup> of the spectral data. The loading vectors for the pH calibration model have a significant feature centered at 6200 cm<sup>-1</sup> (~1610 nm), which is a frequency associated with nitrogen-hydrogen (N-H) bond stretching. A histidine molecule is a likely candidate for the source of N-H vibrational absorption in the spectra, since the hemoglobin molecule possesses 36 histidyl residues, 22 of which are titratable. These protons are known to have a pK<sub>a</sub> of 6.0, which means that they are titratable over the range of pH variation in our samples<sup>9</sup>. We currently believe that the absorption band at about 6200 cm<sup>-1</sup> is associated with the titration of protons on the imidazole ring of the histidyl residues present on the hemoglobin molecule, as shown below.



Thus, it is reasonable to expect that spectroscopic changes will be observed due to the acid-base changes that the histidyl residues undergo. A similar analysis of the source of pH information in the CCD Si array spectra showed that the 590-635 nm region was important to pH prediction in that data. It is known that methemoglobin is very sensitive to pH changes and exhibits changes in its absorption spectrum at approximately 630 nm as it undergoes transition from its acidic to basic chemical forms<sup>10</sup>. Thus, we believe that an important source of pH information in the silicon detector region lies in the acid-base changes of methemoglobin over the pH range studied.

### 2.3.3 pH Determination of Lysed Red Blood Cell Tissue Phantoms using Optical Cuvettes

The ultimate deep tissue pH determination will have to be carried out using a reflectance sampling mode due to the highly light-scattering properties of tissue<sup>3</sup>. If radiation that is

reflected off the second window of the optical flow cell (Fig. 1a) is sampled, the spectral data are significantly changed relative to an experiment where all radiation sampled is a result of scattering from the sample itself. Elimination of reflectance from the second window of the flow cell can be achieved by simply making the cell pathlength greater than the penetration depth of the probe beam. This requires a 1 cm (or greater) pathlength cell. When appropriate cells were tested with whole blood samples we could not, under any flow conditions, get completely satisfactory performance. Slow flow rates resulted in noticeable cell settling, and corresponding spectral shifts. Fast flow rates resulted in channeling (see Section 2.2).

One solution to the problem would be to prepare samples and seal them, with a stir bar, in cuvettes. This approach was tested with whole blood samples. The red blood cells settled when the stirring rate was set below the rate at which cavitation occurred, and the spectral data became impossibly noisy when cavitation occurred. Muscle cells are much larger, by as much as an order of magnitude, than are red blood cells. Thus, the settling problems noted with intact red blood cells would be expected to be magnified with intact muscle cells.

A better solution is to prepare samples with the same chemical composition as tissue, but add a medium that produces a scattering signal nearly identical to that produced by tissue. Such a sample will have identical spectral-feature changes, due to changes in pH, as does tissue. Further, the penetration depth of the optical beam will be identical to that in tissue if the absolute amount of scattering is the same as in a tissue sample. Such a sample, a "tissue phantom", can be prepared by lysing cells to produce the appropriate chemical system, and adding a mixture of microspheres to produce the scattering. Polystyrene microspheres small enough to be easily suspended with low stirring rates produce an appropriate scattering signal<sup>11</sup>.

The initial test of the tissue phantom concept was carried out using a matrix of lysed blood. The pH predictions, and the loading vectors of the calibration model, should be comparable to whole and lysed blood results. These studies were carried out using reflectance spectroscopy, as originally proposed. The samples were sealed in optical cuvettes, which prevents the gas values ( $\text{ppO}_2$  and  $\text{ppCO}_2$ ) from changing and allows the samples to be stored for subsequent studies. This plan was a departure from the original proposal, but we felt that having lysed blood samples in a scattering matrix similar to that of human tissue would have great value toward evaluating the effects of tissue scattering on the quality of pH prediction.

To prepare the lysed blood tissue phantom (LBTP) samples, lysed blood was obtained as described in Section 2.3.2. The LBTP samples consisted of four components: lysed blood, 2% scattering beads (0.042  $\mu\text{m}$  diameter, polystyrene spheres), plasma, and acid or base dissolved in 0.9% saline. We prepared the LBTP samples using an experimental design that was similar to that used for the whole blood sample studies (Figure 2). The concentration of lysed blood in the LBTP samples was held constant in all samples at  $3.73 \pm 0.03 \text{ g Hb/dL}$ , or 20-25% of normal human hemoglobin levels. The reduction in lysed blood concentration was made to closer approximate the levels of blood expected to be present in tissue. The LBTP samples were individually tonometered to the desired pH values, and then measured with the blood gas analyzer. Spectra were collected in reflection using the FT-NIR spectrophotometer equipped with both Si and InSb photodetectors. Given the importance of the spectral information below 670 nm, we had modified our FT-NIR spectrophotometer to use a green HeNe laser reference (543 nm) so that we could record spectra using the FT-NIR Si photodetector between 590-1000 nm. The spectra collected with the FT-NIR InSb detector are shown in Figure 7.

The LBTP cuvettes possessed a constant scattering matrix, so the magnitude of baseline variation is small. The 2% scattering bead concentration was used based on an experiment in which variable scattering cuvettes (1.6-2.4%) were compared with FT-NIR reflectance spectra of the human forearm from 10 different subjects. Figure 8 shows the spectra of the variable scatter tissue phantoms (lower set of spectra) together with the spectra from the human subjects (several replicate spectra for each subject). The two sets of spectra actually overlap, but have been offset for clarity. The same water band peak-to-trough ratios exist in both sets of data, and the amount of baseline variation is remarkably similar. Consequently, we feel confident that the tissue phantoms are an excellent surrogate for a human tissue matrix and that a scattering concentration of 2% represents a good estimate for the average level of scatter in human tissue..

The spectral data obtained from the set of cuvettes was modeled using the PLS algorithm. The pH calibration obtained from the InSb detector (spectral range to 1500-1800 nm) yielded a SEP of 0.038 pH units, which is shown in Figure 9. The loading vectors generated by the PLS calibration show features nearly identical to those seen in the whole and lysed blood studies, an indication that the pH model is based on identical chemical changes in the samples. The calibration results obtained from the silicon detector were poor, having an SEP of 0.085 pH units. The detector had drifted significantly during the course of the experiment. This detector was found to be faulty and sent to the manufacturer for repair.

## 2.4 DEVELOP PROCEDURE FOR PREPARING MUSCLE CELL SUSPENSIONS (TASK 4)

This set of experiments was carried out using tissue phantoms, but prepared with a muscle cell homogenate rather than lysed blood. To prepare the muscle homogenate, fresh lean beef muscle was obtained from a commercial slaughterhouse. Muscles were dissected free of connective tissues, diced by hand, and homogenized with a Waring blender in 0.9% sodium chloride irrigation USP solution. Only enough saline was used to create a viscous homogenate. Specimens were placed in 50 ml centrifuge tubes and were spun at 3000 rpm for 15 minutes in an IEC 7R refrigerated centrifuge. Tubes were removed, muscle supernatant was pipetted into flasks, and the flasks were stored at 4°C. Precipitates containing non-homogenized fragments of muscle, the cell walls, and connective tissue were discarded. The resulting muscle cell suspension was brought to physiological pH and bicarbonate concentration levels by the addition of sodium hydroxide and sodium bicarbonate as required. Using a muscle cell suspension prepared as described above, we found that we could successfully tonometer the suspension to desired pH values. The Sigaard-Anderson base excess model was used to predict the amounts of acid or base to add to the suspension prior to tonometry.

## 2.5 DETERMINE pH OF MUSCLE CELL SUSPENSIONS (TASK 5)

Our original proposal for measuring pH in the muscle cell suspensions was similar to that for blood samples. We modified our proposal to be similar to that for preparing the LBTP samples, for the reasons stated above.

### 2.5.1 *pH Determination of Muscle Cell Tissue Phantoms*

In our initial muscle cell study we prepared 31 muscle cell tissue phantom (MCTP) cuvette samples over a range of pH values, analogous to the LBTP cuvette samples. The pH was

varied by tonometering the samples to various amounts of ppCO<sub>2</sub> after adding a given amount of acid or base. Thus, the bicarbonate buffer system was adjusted to reach the target pH values. The experimental design for the MCTP samples included randomizing the order of sample preparation and orthogonalizing pH and other muscle cell suspension variables (such as bicarbonate ion concentration). This orthogonal experimental design ensures that pH prediction cannot be based on spurious correlation to variation in one of the other muscle sample variables. The MCTP cuvette samples (31 total) span a range of pH values (6.8 - 8.0), and they consist of 70% muscle cell suspension, 21% solution of scattering beads (9.5% concentration), and a 9% mixture of acid or base and saline. The final bead concentration was 0.02 g/ml (2%) and the diameter of the beads was 0.042 µm (polystyrene spheres). The samples were sealed in 1 cm optical cuvettes that also contained a magnetic stirbar.

Each sample was immediately measured with the reflectance FT-NIR spectrophotometer while being stirred by the magnetic stirrer at 300 rpm. Spectra were collected from both the Si and InSb photodetectors. The spectra from the FT-NIR InSb detector are shown in Figure 10. The general appearance and quality of the spectra appear similar to the FT-NIR InSb reflectance spectra from the lysed blood tissue phantoms (see Figure 7). The spectra obtained from the FT-NIR Si detector are shown in Figure 11. A calibration model based on the spectral data and the reference pH values was generated using the PLS algorithm. The InSb spectral data taken between 1500-1850 nm yielded pH prediction having a cross-validated SEP of 0.045 pH units (see Figure 12). This result was obtained after removing four outlier samples, which all had large pH prediction errors. The Si spectral data achieved a pH cross-validated SEP of 0.045 pH units, using the spectral region between 580-870 nm (see Figure 13). All 31 samples were used in the calibration.

This first MCTP sample study showed that the muscle homogenate could be successfully tonometered to the target pH values over the pH range of 6.8-8.0. Clinically important levels for pH prediction were obtained from both FT-NIR detectors. However, this muscle cell suspension was not as stable as was the lysed blood samples. Three out of the four outlier samples removed from the FT-NIR InSb data set had a significant color change. These samples had been left at room temperature for a considerable length of time, a fact we now know is detrimental to muscle cell suspensions. We concluded that tissue phantom samples made from this muscle cell suspension appear to be stable for about one day, compared with five days for the lysed blood tissue phantom samples. We felt that these results were encouraging but that further studies were necessary to confirm the results that we had obtained.

### ***2.5.2 pH Determination of Muscle Cell Tissue Phantoms with NMR Validation***

Based on the results presented in Section 2.5.1, we decided to execute further studies to answer questions regarding the stability of the muscle cell homogenate that was used in preparing the MCTP samples. This additional research also sought to expand the range of pH variation of the muscle homogenate and to verify the validity of using the ABG instrumentation as a reference pH methodology. The viability and stability of the muscle homogenate was planned to be assessed, in part, using nuclear magnetic resonance (NMR) spectroscopy, which is well known as an *in vivo* method for determining tissue pH<sup>12-14</sup>. The NMR work is beyond that originally planned in the Phase I research proposal. We felt, however, that this additional effort was necessary to conclusively demonstrate the feasibility of a deep tissue pH monitor.

The stability of the muscle homogenate used in the MCTB samples came into question with the discovery of several outlier samples in the data set that partially correlated with a color change in the muscle homogenate preparation. To definitively answer the question of stability, we made two batches of bovine muscle homogenate. The first batch was made from fresh lean beef that was stored for four days at 4°C before preparing the muscle homogenate, while the second batch was made from fresh lean beef that was obtained and processed within five hours after slaughter from a commercial slaughterhouse. The first batch was pre-processed by removing the gross fat from the muscle tissue, which was then minced. The minced lean beef was then given to the UNM Anatomy Department, where the final muscle homogenate was prepared as described in Section 2.4. The second batch was pre-processed by removing the gross fat as before but was then passed through a meat grinder. The homogenate was prepared as described in Section 2.4 with the following exceptions: (1) less saline was needed for the blending process because of the meat grinding process (homogenate was more concentrated), (2) the tissue was blended under a nitrogen purge to minimize the possibility of oxidation, and (3) once received from the Anatomy staff, we collected the muscle homogenate from the bottom of the container leaving behind the top 10% of the homogenate which contained visible amounts of lipid.

The range of pH variation of the samples was expanded to include the low pH values that are possible during heavy exercise and especially during conditions leading to tissue ischemia. The protocol used to achieve the target pH values, between 6.2 and 7.6, had to be changed from that used in the prior studies because the lowest pH values cannot be achieved using CO<sub>2</sub> as the acid. We decided to use lactic acid additions to drive the pH to low values and sodium hydroxide to drive the pH to high values. Following addition of the acid or base, we tonometered a given sample for five minutes at ambient conditions to force all of the CO<sub>2</sub> gas out of the sample (the atmosphere contains only 0.25 mmHg ppCO<sub>2</sub>). By driving off nearly all of the CO<sub>2</sub>, we were assured that the bicarbonate buffer system was inactivated. We hypothesized that the phosphate buffer systems would now be the dominate buffering system in the muscle homogenate, since there was little or no hemoglobin (Hb) present in the muscle homogenates (Hb levels were below the sensitivity limit of a commercial co-oximeter).

We prepared only 15 tissue phantom samples using the first batch of muscle homogenate. The target pH values were achieved without any difficulty, the pH values being determined from the ABG instrumental measurements. We obtained the <sup>31</sup>P NMR spectra from 12 of the samples. The NMR spectra we obtained differed from what has been published in the literature<sup>12-14</sup>. The literature on <sup>31</sup>P NMR of muscle maintains that a phosphocreatine (PCr) band should be evident in the NMR spectra, and its chemical shift should be invariant to pH changes of the sample. Hence, it serves as an internal marker for chemical shifts in other bands. The literature also states that the inorganic phosphate NMR bands will be very sensitive to sample pH changes. In fact, the chemical shifts of the inorganic phosphate (P<sub>i</sub>) bands are directly proportional to pH changes in the samples. The tissue phantom samples we prepared exhibited a large phospholipid band in the NMR spectra and no apparent P<sub>i</sub> or PCr bands. We concluded from these results that the first batch of muscle homogenate was not viable, since it did not exhibit the P<sub>i</sub> and PCr NMR bands that are associated with healthy, normal muscle.

We then prepared 60 tissue phantom samples using the second batch of muscle homogenate (MCTP2). The range of pH variation in the 60 samples spanned 6.03-7.65 pH units. FT-NIR reflectance spectra were collected using both the Si and InSb detectors, similar to the

MCTP and LBTP sample sets. We obtained the  $^{31}\text{P}$  NMR spectra of 10 of the samples. These samples were selected such that they spanned the range of pH variation present in the entire data set. The NMR spectra obtained from these 10 samples are shown in Figure 14. The phospholipid NMR bands were not observed in any of the spectra, and we now observed strong NMR peaks that corresponded to the  $\text{P}_i$  and  $\text{PCr}$  features reported in the literature<sup>12-14</sup>. However, Figure 14 does show that the  $\text{PCr}$  peak intensity does decrease as the pH is lower, which has been observed<sup>15</sup>. Figure 14 shows that the  $\text{PCr}$  peak at -2.5 ppm chemical shift does not shift as the pH of the samples is varied. However, as expected, the  $\text{P}_i$  peak between 1.0-4.0 ppm chemical shift exhibits an obvious dependence on the sample pH. These results are analogous to literature results obtained from normal muscle.

To verify the accuracy of the ABG reference pH measurement that we had obtained for the MCTP2 samples, we calculated the pH<sup>16</sup> of the 10 NMR samples and compared it to the pH determined from the ABG instrument for the same 10 samples. A plot of the ABG pH vs. the NMR pH is shown in Figure 15, which shows that the two methods agree extremely well. The two reference methods show slight differences at the upper and lower pH values, but this could be caused by the fact that the NMR pH values were calculated from an equation in the literature relating pH and chemical shift<sup>16</sup>. The SEP of the ABG pH values from the NMR pH identity line is 0.033 pH units. These results confirmed that the ABG pH measurement is a valid pH reference standard.

The FT-NIR InSb spectra that were collected for the MCTP2 samples are shown in Figure 16, and the FT-NIR Si spectra are displayed in Figure 17. Using partial least squares calibration as before, the FT-NIR spectra were calibrated against the ABG pH reference values. The SEP for the FT-NIR InSb data was 0.042 pH units when calibrated over the  $5400\text{-}6667\text{ cm}^{-1}$  spectral region (1500-1850 nm). Using the FT-NIR Si spectral data, the SEP was 0.049 pH units when calibrated over the  $14690\text{-}17222\text{ cm}^{-1}$  spectral region (580-680 nm). These results are plotted in Figures 18 and 19, respectively.

A chemometrics analysis of the spectral data to discover what spectral features were important for determining pH was done in a manner identical to that described for the lysed blood samples in Section 2.3.2. The source of spectroscopic variation correlating to pH in the FT-NIR InSb spectra appears remarkably similar to that observed in the lysed blood samples (see Section 2.3.2). This similarity indicates that the histidine molecule absorptions are also responsible for pH predictions in muscle suspension preparations, which is reasonable since myoglobin is present in muscle and it possesses histidyl residues analogous to hemoglobin. A similar chemometrics analysis of the FT-NIR Si data showed spectral features that were similar to the methemoglobin features observed in the lysed blood pH loading vectors. For muscle samples, these spectroscopic features would indicate that metmyoglobin is responsible for pH prediction. It is reasonable that the pH loading vectors should look similar since myoglobin and hemoglobin have similar visible absorption spectra.

### 3. CONCLUSIONS

Phase I research has demonstrated the proof-of-principle for measuring deep tissue pH using NIR/VIS spectroscopy and chemometrics. Our approach to researching the issues involved in the determination of deep tissue pH has been systematic, building on the knowledge gained from each experiment we executed. We began our Phase I research by investigating the spectroscopic requirements for successful pH prediction in whole blood, based upon the fact that blood is present in tissue and can be readily pH-adjusted. From this initial investigation, we learned that pH prediction was possible, but we could not clearly elucidate the source of pH information in the spectra due to relatively large baseline variations caused by variations in cell sizes. These facts prompted us to investigate lysed blood samples, from which we not only achieved pH prediction, but also successfully identified the pH spectral information. We identified two sources of pH information in the spectroscopic data: acid-base changes in the histidyl residues of hemoglobin and acid-base changes in methemoglobin. These features were discernible in the NIR (1500-1800 nm) and visible (580-680 nm) portions of the spectral data of all subsequent studies. We next prepared lysed blood tissue phantom cuvettes to evaluate whether pH prediction could be maintained in a highly scattering medium similar to human tissue. The tissue phantom optical cuvettes for lysed blood were almost identical, spectroscopically, to FT-NIR reflectance spectra of human tissue. Even in the presence of a scattering matrix, lysed blood pH was successfully predicted to clinically useful values (standard error of prediction of 0.03 pH units).

This knowledge base in lysed blood positioned us to perform the critical experiments that would determine whether or not non-invasive deep tissue pH prediction was possible. Bovine muscle cell homogenate (lysed muscle) was prepared and mixed with a scattering matrix to yield muscle cell tissue phantoms, analogous to the lysed blood tissue phantoms. The pH of these muscle cell tissue phantoms was determined with SEP results less than 0.05 pH units, but questions regarding sample viability and our reference pH measurements were present upon evaluation of the data. A second bovine muscle cell tissue phantom sample set was prepared in which NMR measurements were made on a subset of the samples. The NMR results showed that the homogenate contained signals observed in healthy, normal muscle, indicating that the homogenate was viable. NMR pH measurements for the subset of 10 samples agreed well with the arterial blood gas measurements, yielding an SEP of 0.033 pH units between the two reference measurements. Partial least squares calibration of the FT-NIR InSb and Si spectral data sets for the second muscle cell tissue phantoms yielded SEP values of 0.042 and 0.049 pH units, respectively. The source of spectral pH information was also identified for these samples, which was the acid-base changes of the metmyoglobin and of the histidyl residues on myoglobin, similar to the information seen with the lysed blood tissue phantom samples.

These results are clinically relevant determinations of pH, they have been achieved in a scattering matrix similar to human tissue, the reference pH method was verified, and the source of information responsible for pH prediction was identified. Based on these results, we conclude that non-invasive deep tissue pH measurement is feasible using FT-NIR spectroscopy and chemometrics. Based upon the promising results thus far achieved, our goal is to continue this investigation under a Phase II research program.

#### 4. REFERENCES

1. Takano, et al., *J. Pediatric Surgery*, **28**, 1376 (1993).
2. Martens and T. Naes, *Multivariate Calibration*, Wiley & Sons, Chichester, 1989.
3. Duck, Francis A., "Physical Properties of Tissue: A Comprehensive Reference Book," Ch. 3, Academic Press, London (1990).
4. Sigaard-Anderson, O., *Ann. NY Acad. Sci.*, **133**, 41 (1966).
5. Loepky, J.A., et al., *Respiration Physiology*, **94**, 109-120 (1993).
6. Pennell, Robert E., "Composition of Normal Human Red Cells," in "The Red Blood Cell: A Comprehensive Treatise," Charles Bishop and Douglas M. Surgener, eds., Ch. 2, pp. 29-62, Academic Press, New York (1964).
7. Widdas, W.F. and G.F. Baker, *J. Physiology*, **459**, 385P (1993).
8. Gary-Bobo, C.M. and A.K. Solomon, *J. Gen. Physiology*, **52**, 825 (1968).
9. Tanford, C. and Y. Nozaki, *J. Biol. Chem.*, **241**, 2832 (1966).
10. Wittenberg, J.B., et al., *Proc. Natl. Acad. Sci. U.S.*, **67**, 1846 (1970).
11. Flock, S.T., et al., *Med. Phys.*, **14**, 835 (1987).
12. Sapega, et al., *Medicine & Science in Sports & Exercise*, **19**(4), 410-20 (1987).
13. Labotka, *Biochemistry*, **23**, 5549-55 (1984).
14. Moon and Richards, *J. Biological Chemistry*, **248**(20), 7276-7278 (1973).
15. Sullivan, et al., *J. Applied Physiology*, **77**(5), 2184-2200 (1994).
16. Pettegrew, et al., *Magnetic Resonance Imaging*, **6**, 135-142, (1988).

# Sample Delivery Subsystem

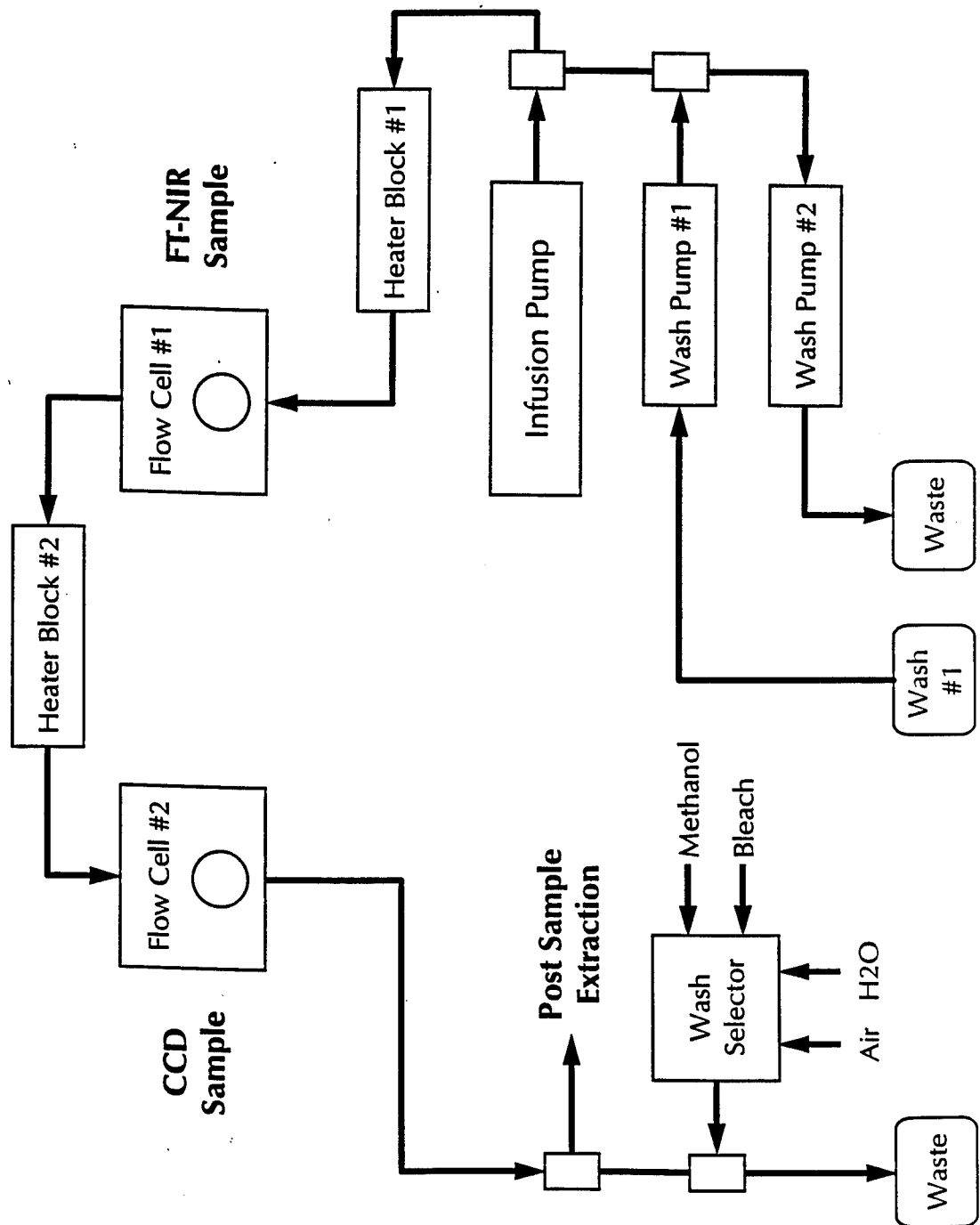


Figure 1a

# Environmental Control Subsystem

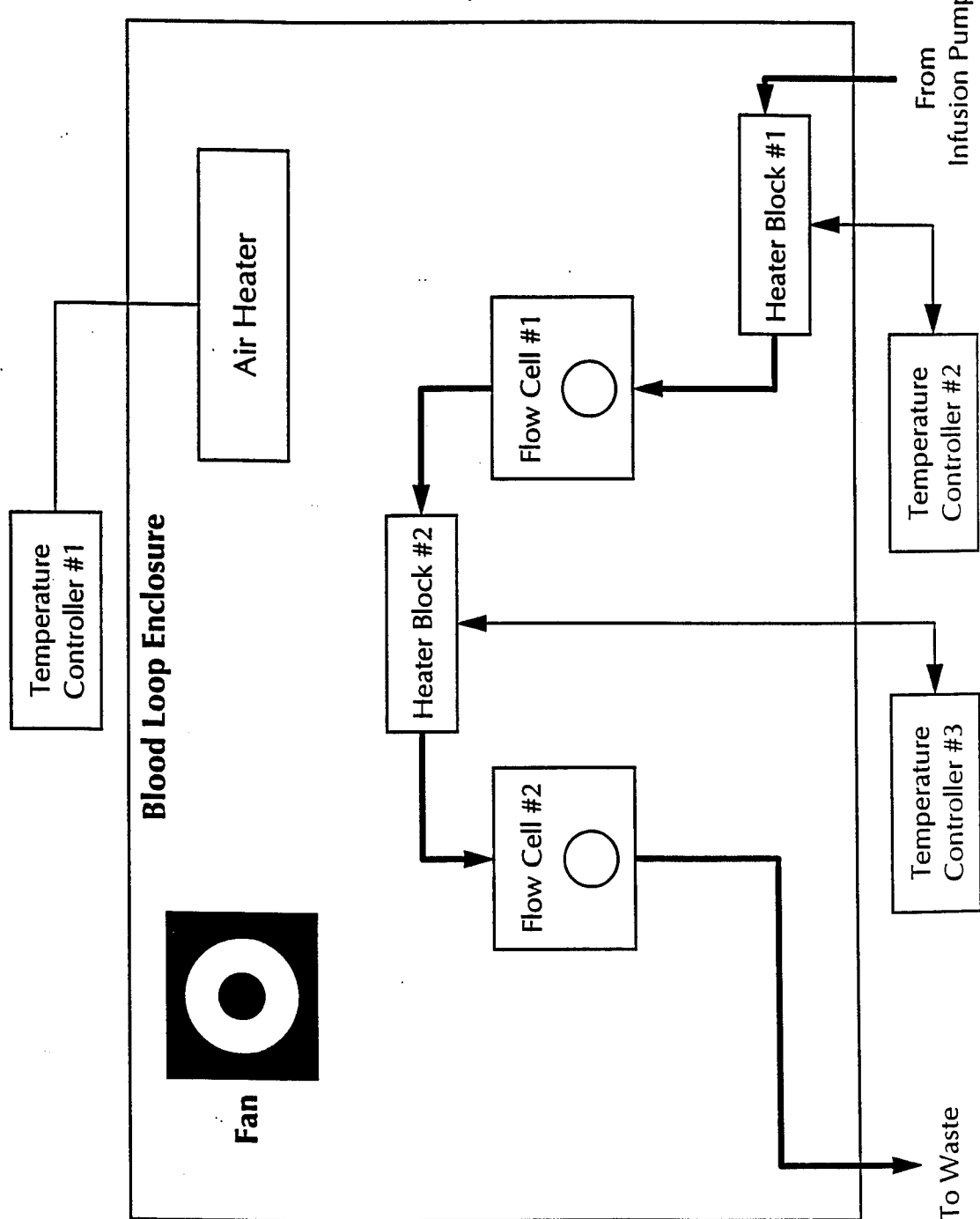


Figure 1b

## Experimental Design for Intact Red Blood Cell Samples

FIGURE 2

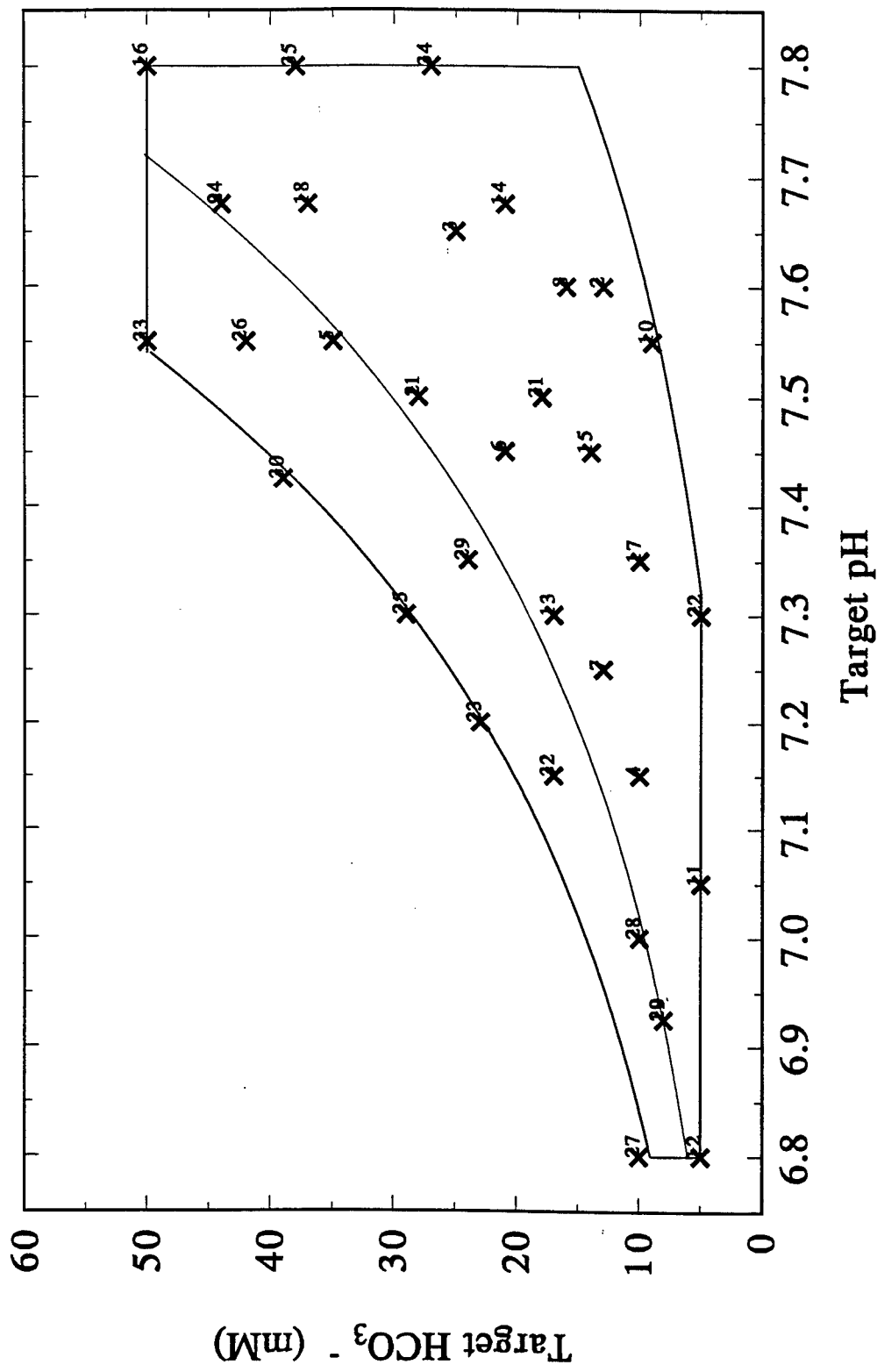




Fig. 3. FT-NIR InSb Absorbance Spectra Of Intact Red Blood Cells

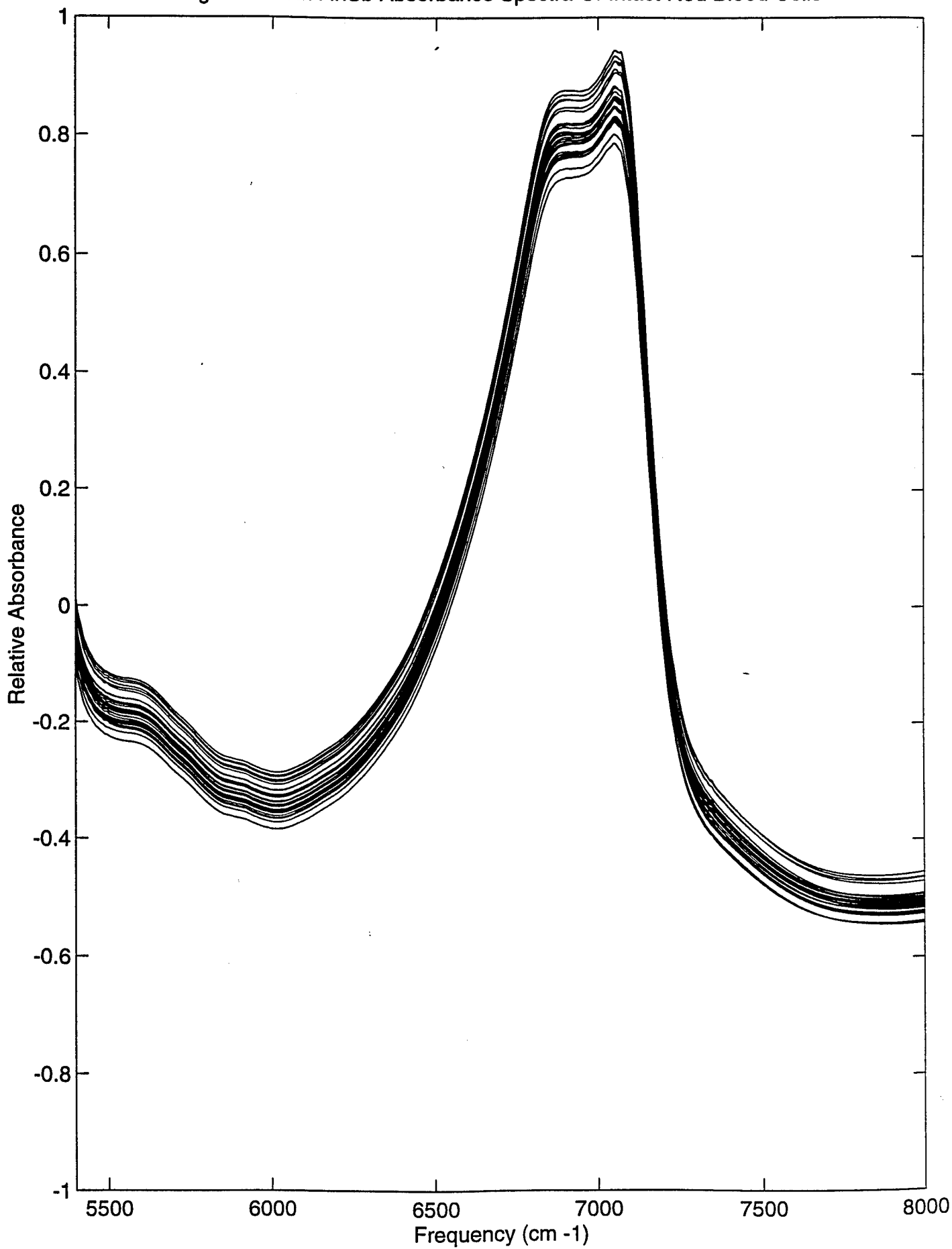


FIGURE 4

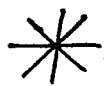
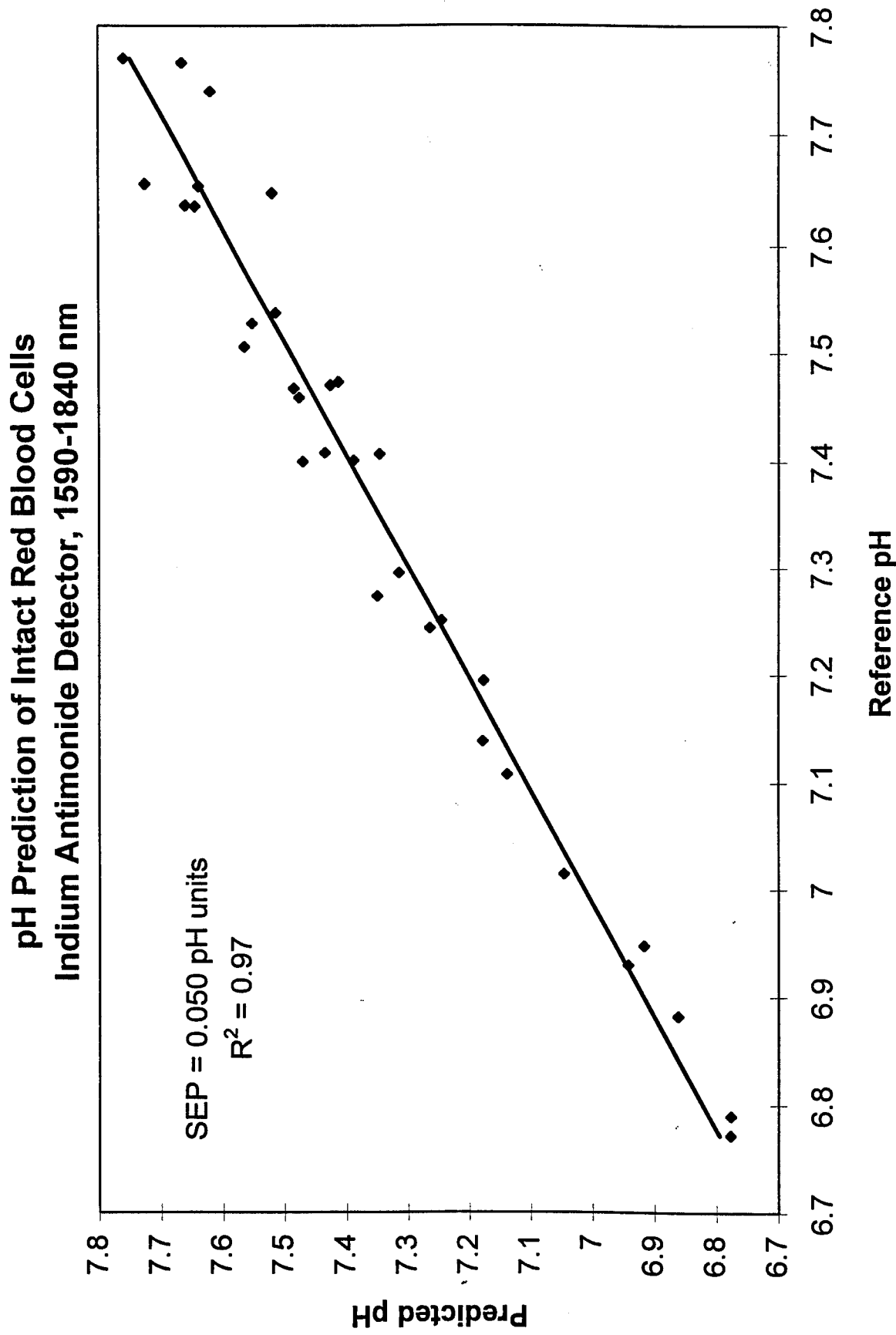




Fig. 5. FT-NIR InSb Absorbance Spectra Of Lysed Red Blood Cells

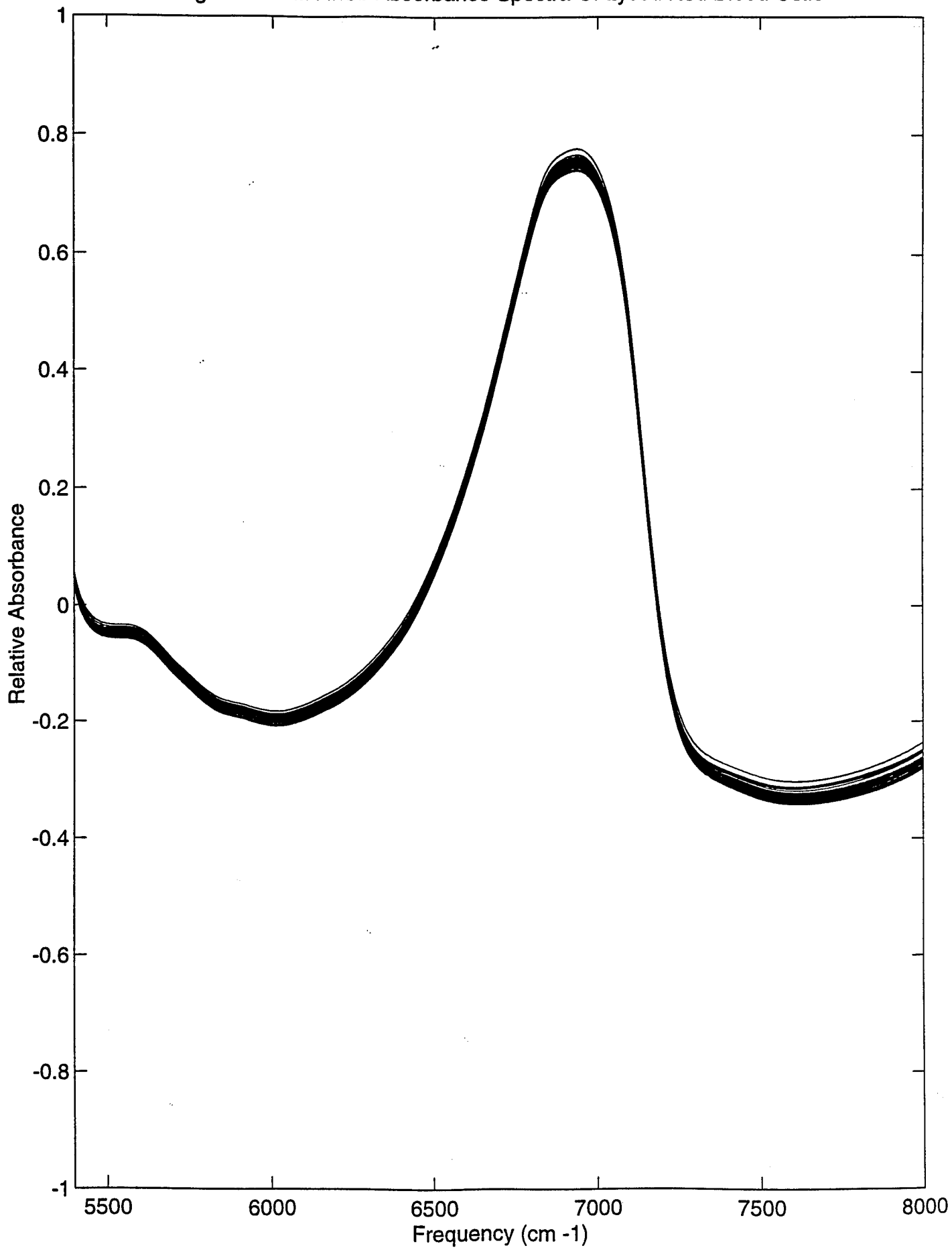


FIGURE 6

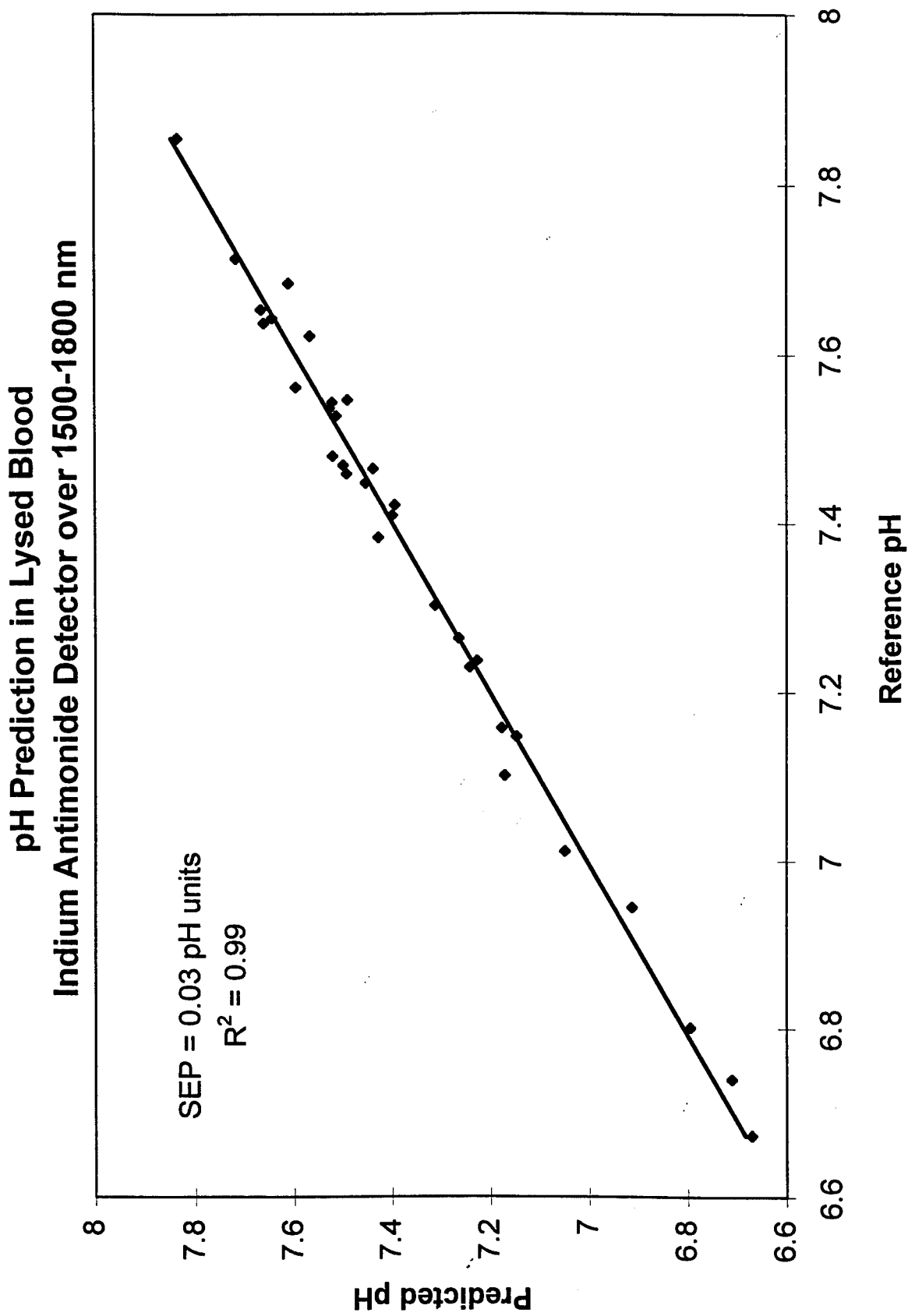
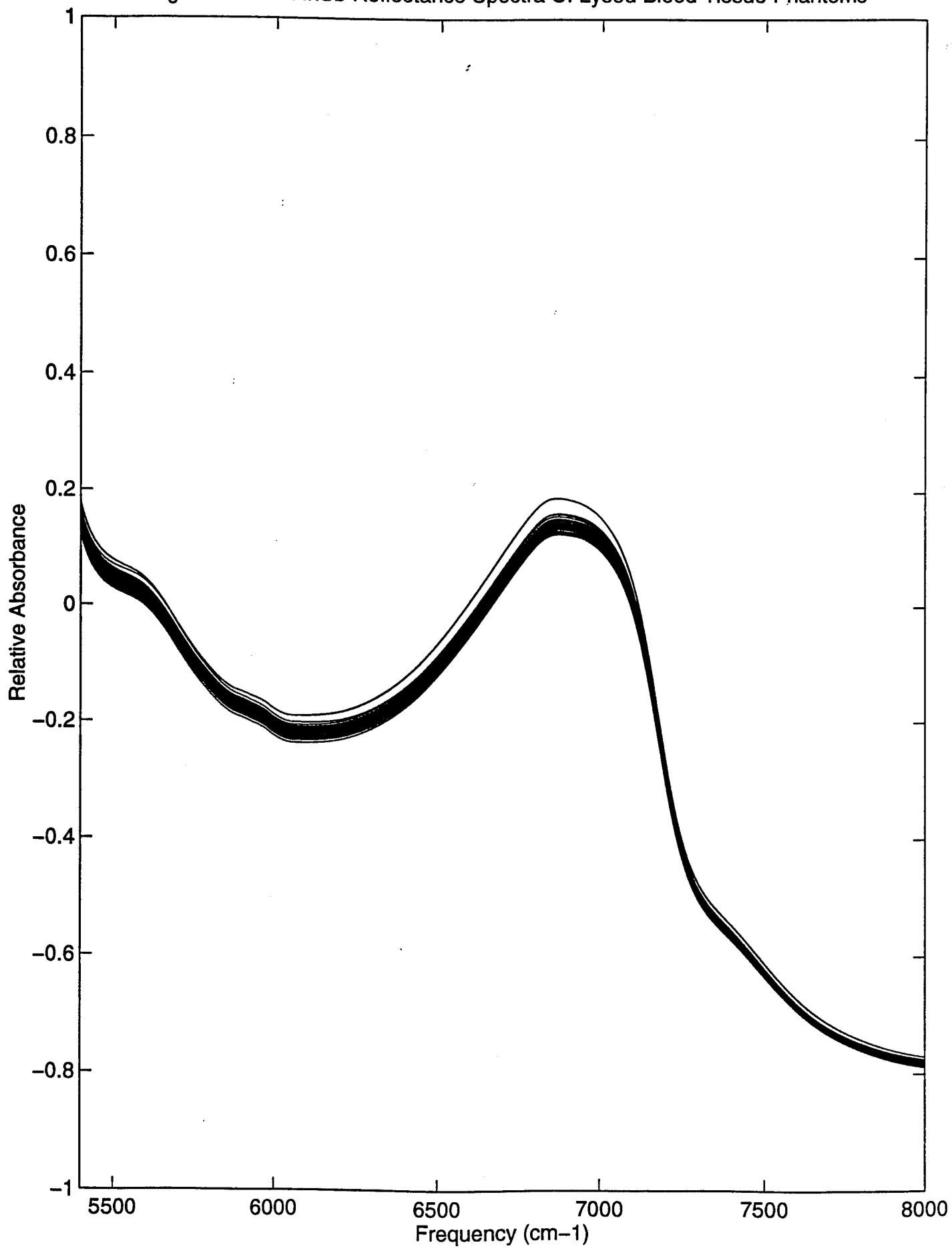


Fig. 7. FT-NIR InSb Reflectance Spectra Of Lysed Blood Tissue Phantoms



## FT-NIR Reflectance Spectra of Scattering Samples:

Human Forearm (10 patients, replicate spectra, top curve)

vs. Variable Scattering Tissue Phantoms (1.6-2.4%, bottom curve)

Figure 8

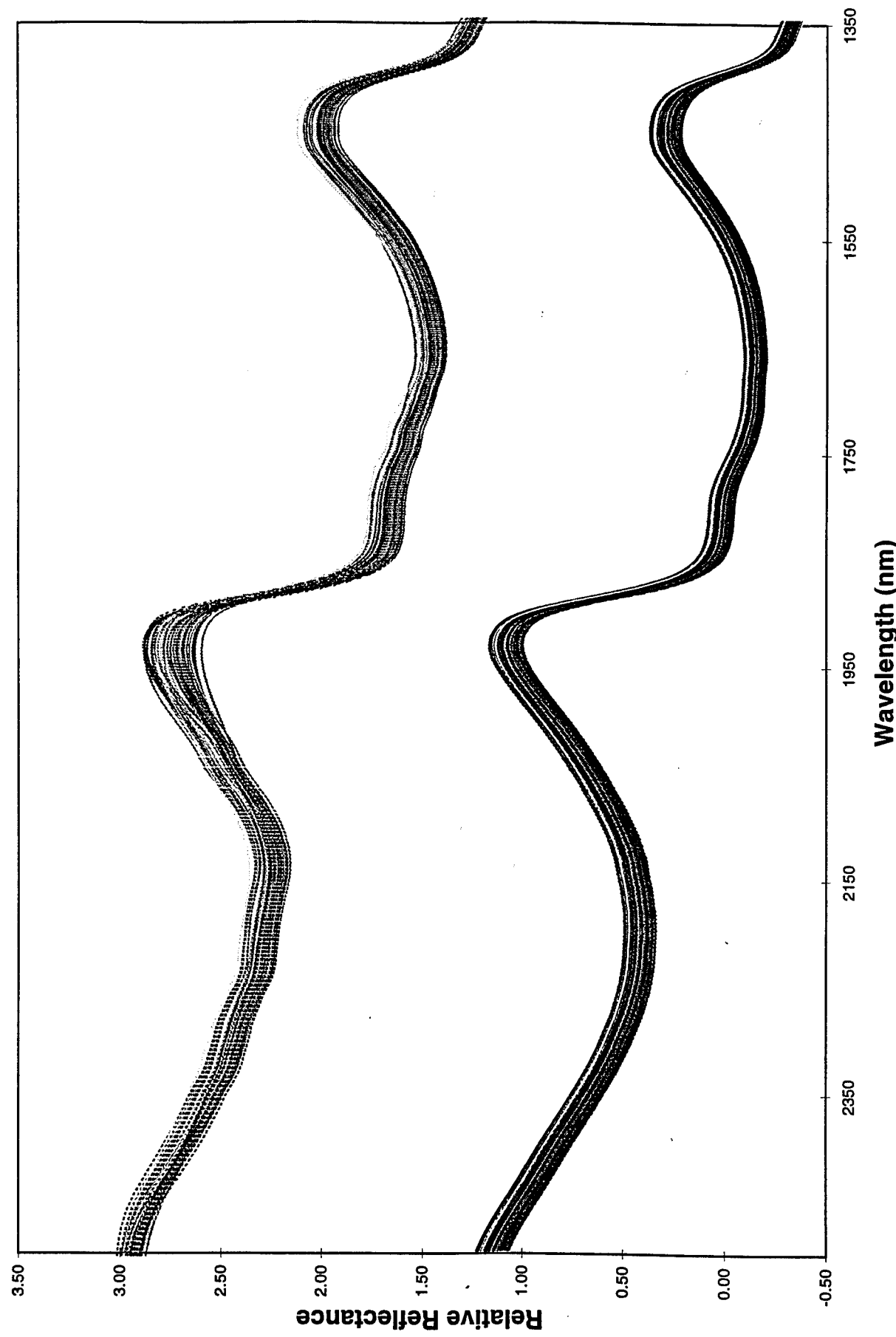


FIGURE 9

pH Prediction in Lysed Blood Tissue Phantoms  
Indium Antimonide Detector over 1500-1850 nm

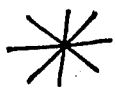
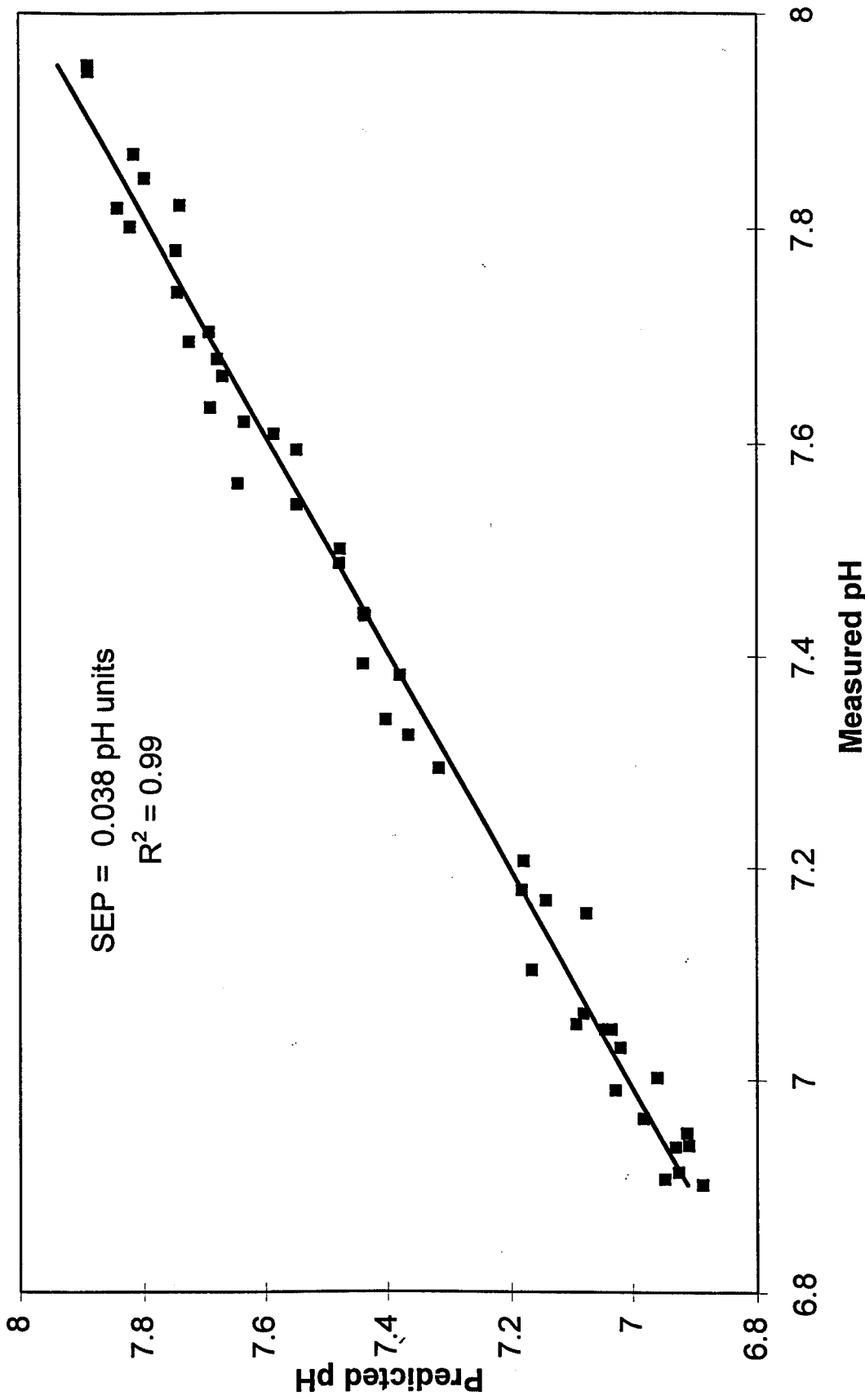


Fig. 10. FT-NIR InSb Reflectance Spectra Of Muscle Cell Tissue Phantoms

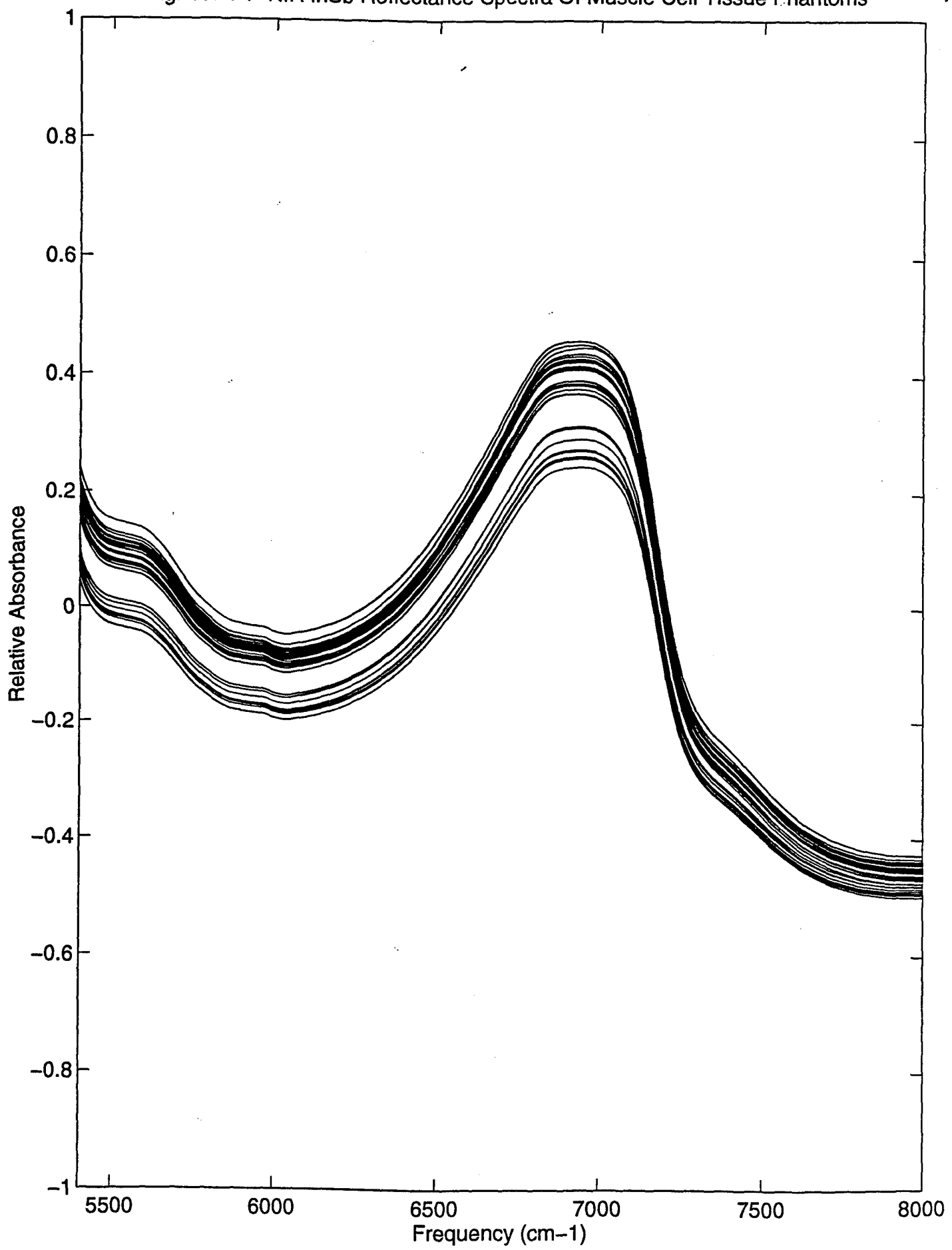
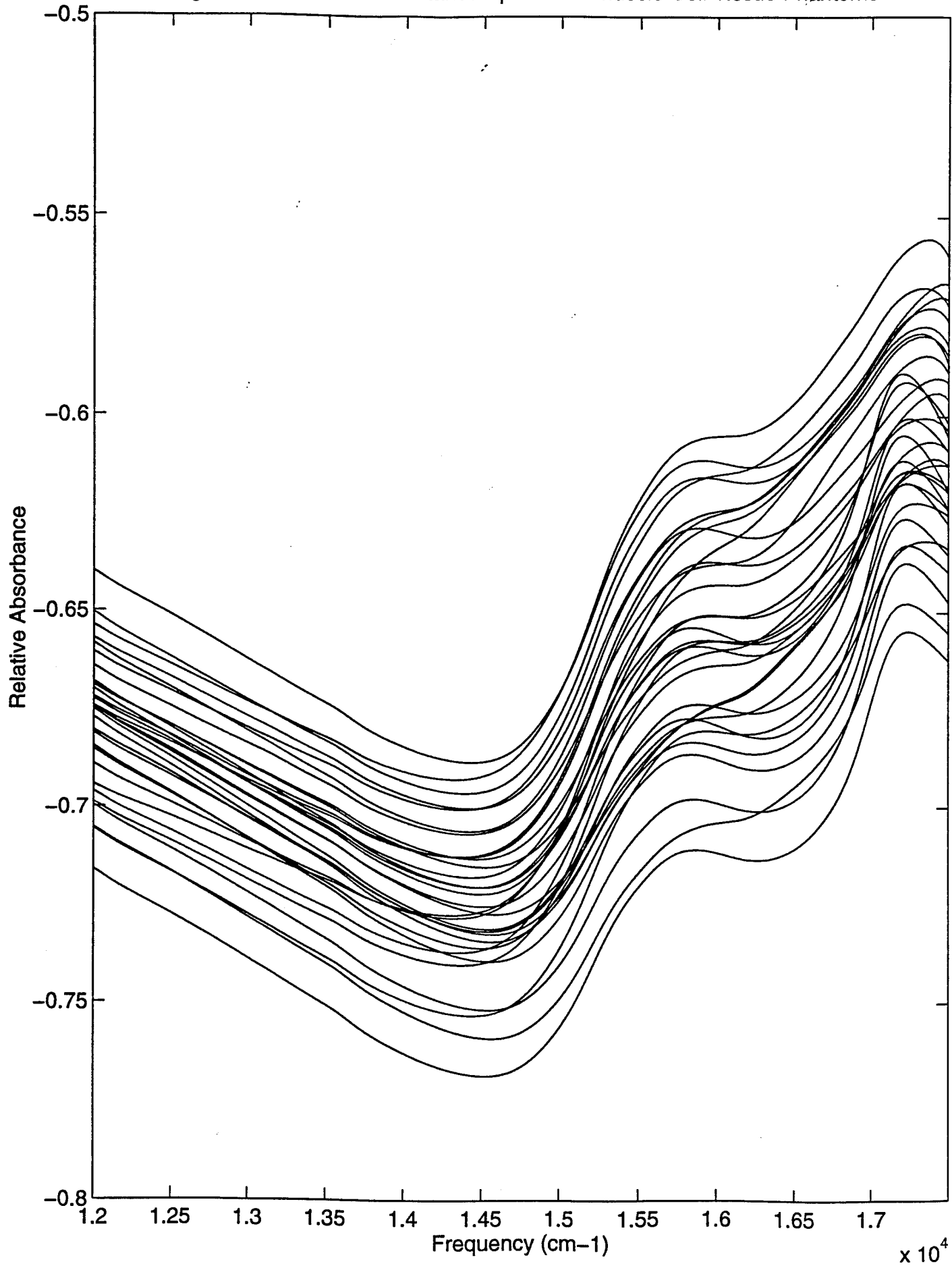


Fig. 11. FT-NIR Si Reflectance Spectra Of Muscle Cell Tissue Phantoms



**pH Determination in Muscle Tissue Phantoms (MCTP)**  
**Indium Antimonide Detector over 1500 - 1850 nm**

**FIGURE 12**

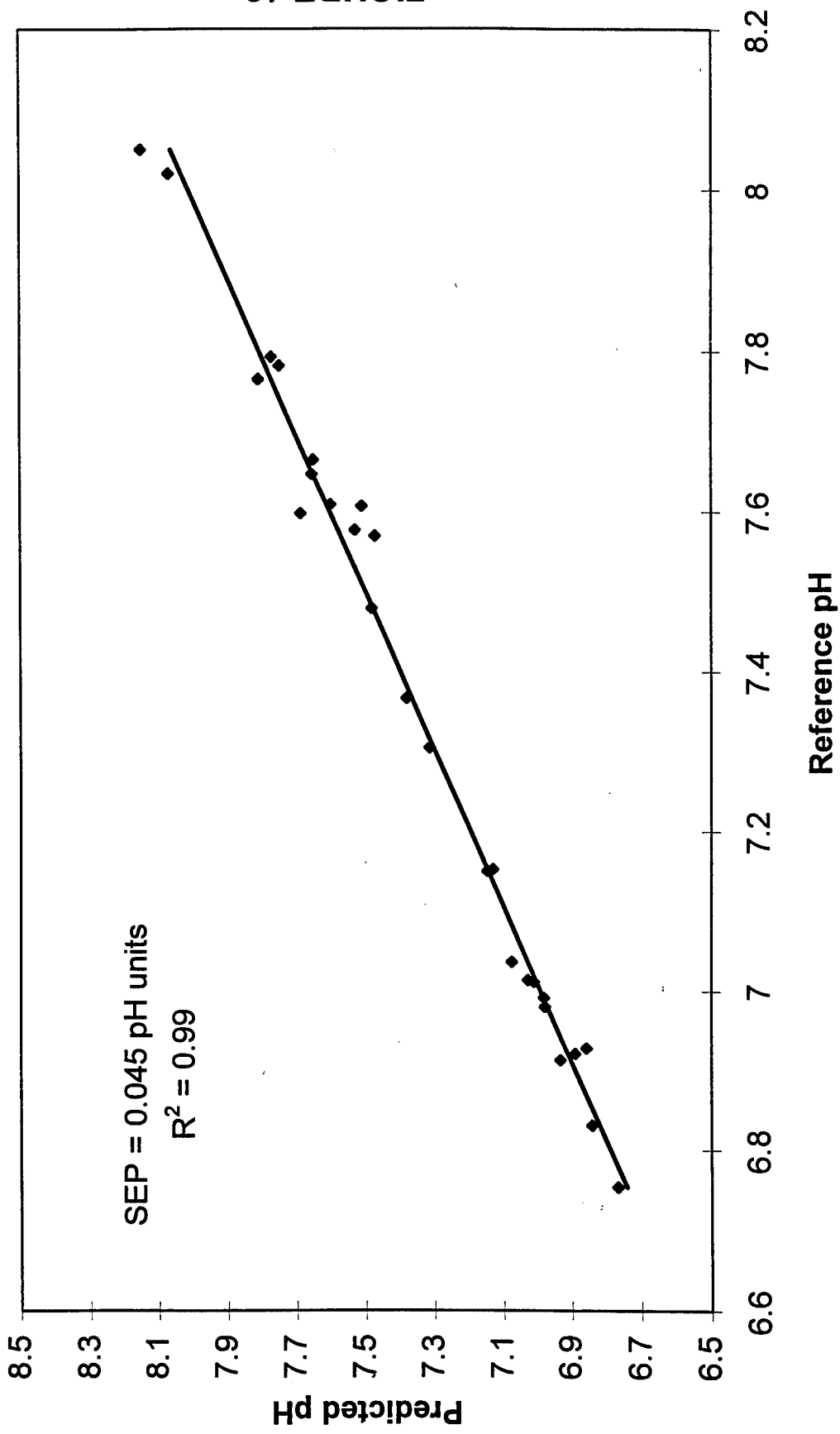
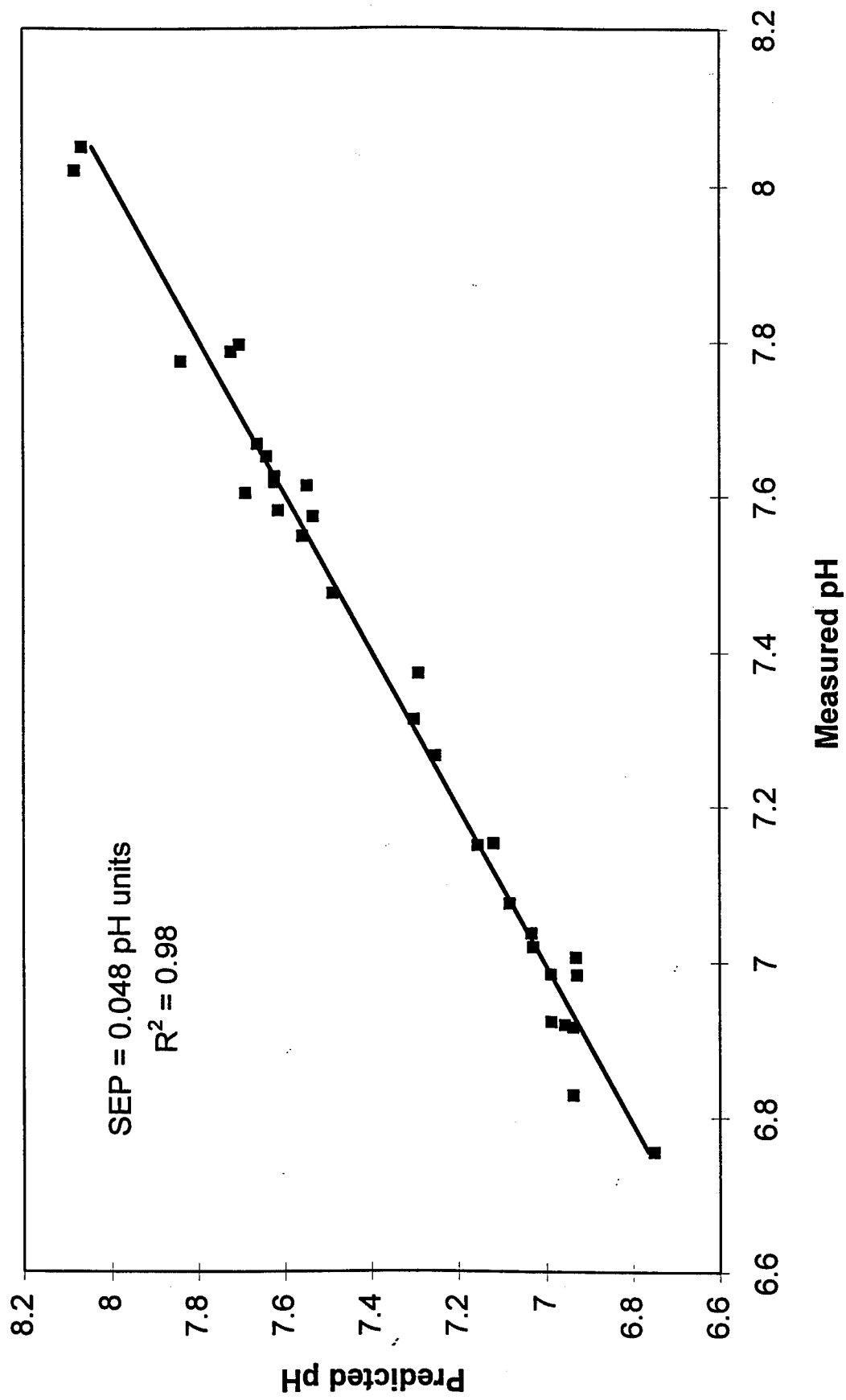


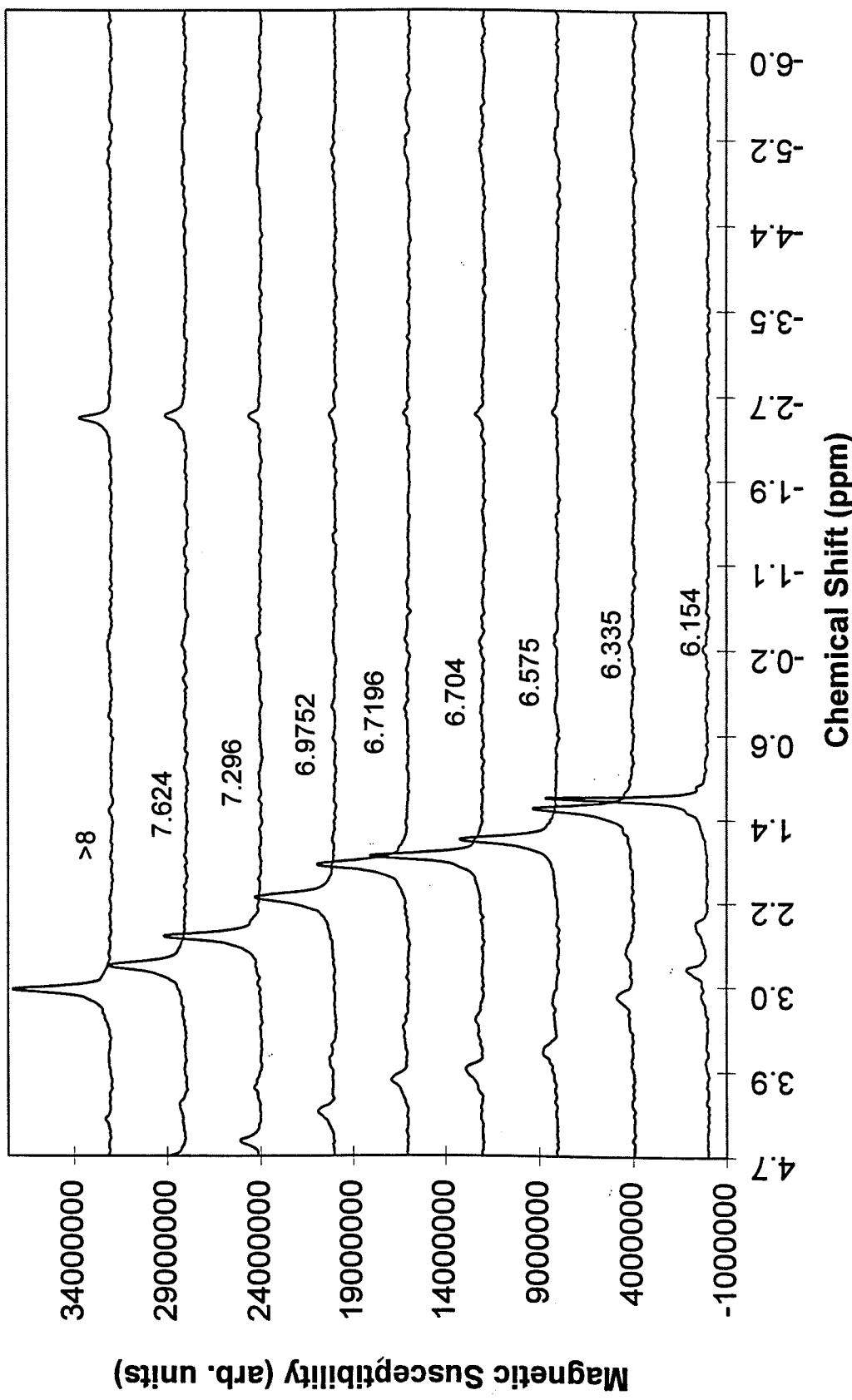
FIGURE 13

pH Prediction in Muscle Cell Tissue Phantoms (MCTP)  
Silicon Detector over 580 - 870 nm



**NMR Shift with pH Variation  
Muscle Cell Tissue Phantom Samples (MCTP2)**

**FIGURE 14**



**Comparison of pH Reference Methodologies**  
**ABG pH vs. NMR pH**

SEP = 0.033 pH units  
 $R^2 = 0.999$

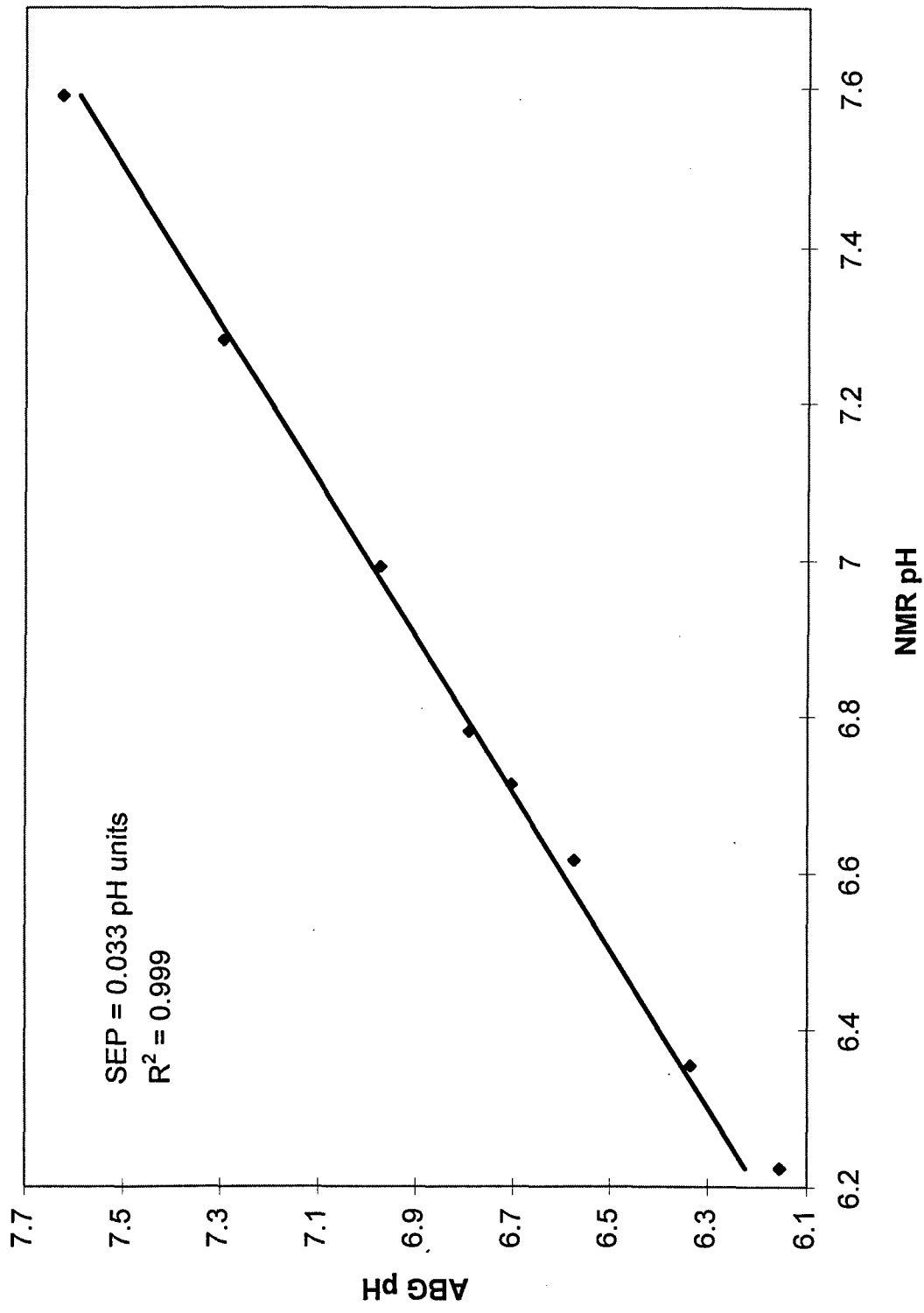


Figure 15



Fig. 16. FT-NIR InSb Reflectance Spectra Of Muscle Cell Tissue Phantoms

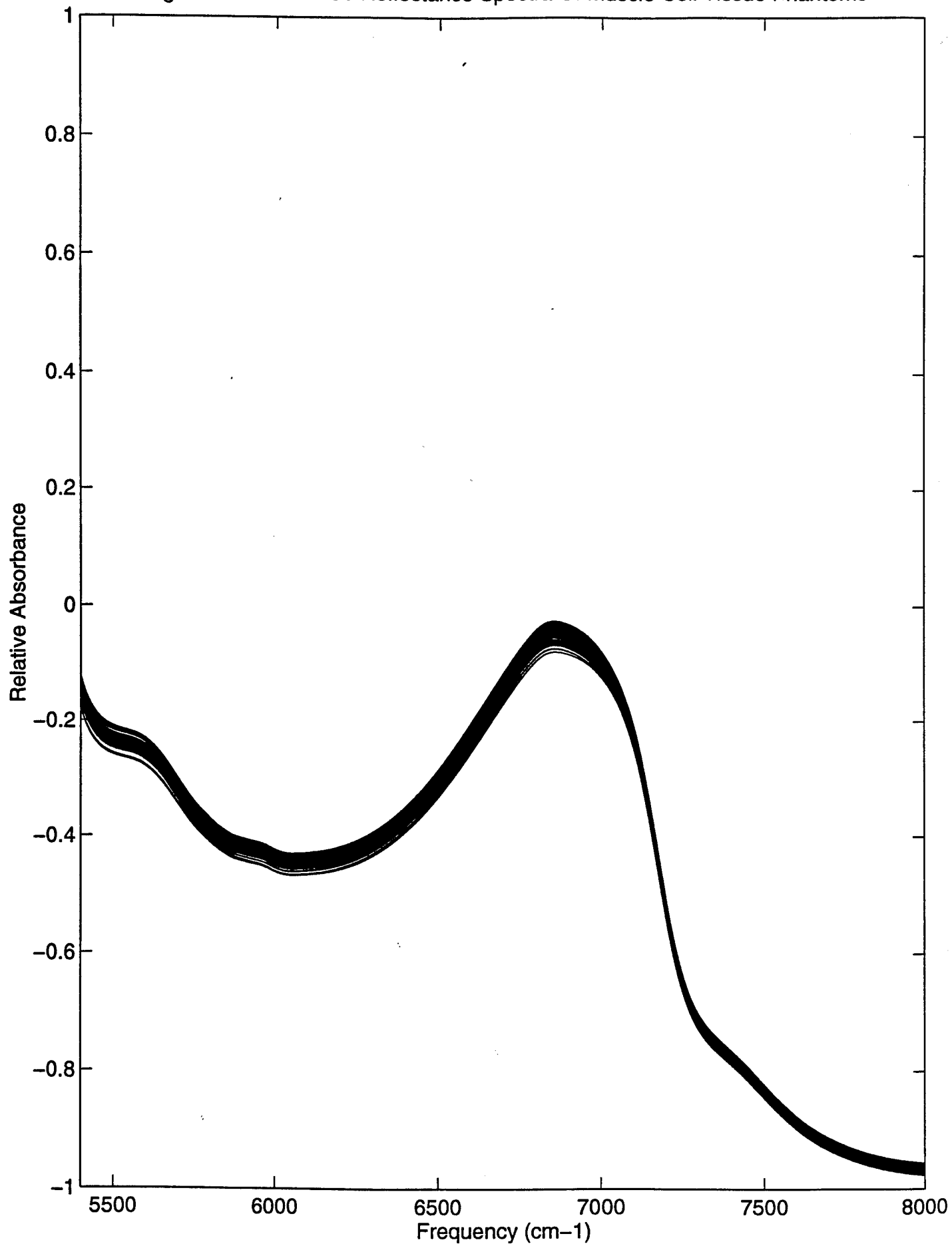
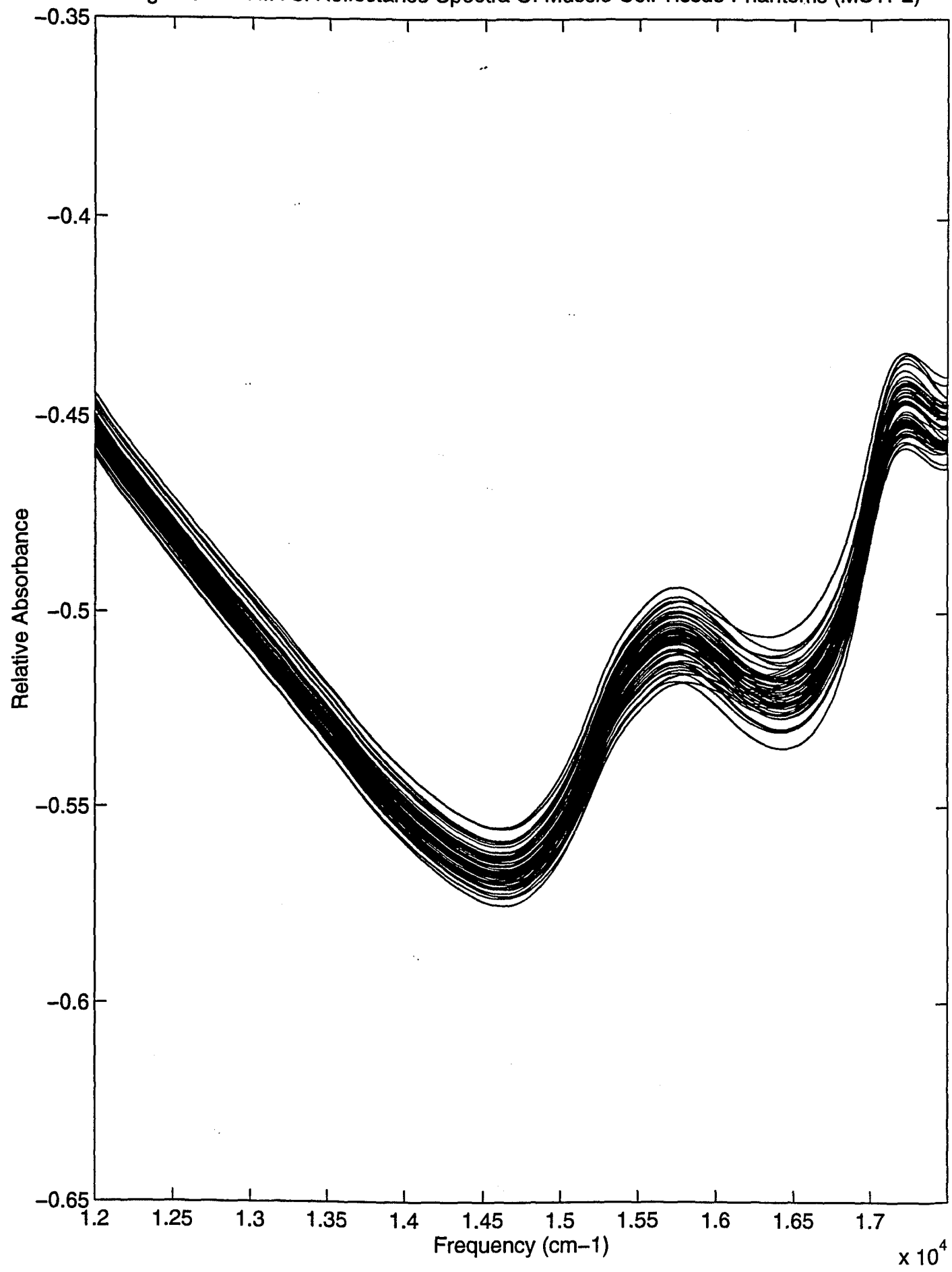
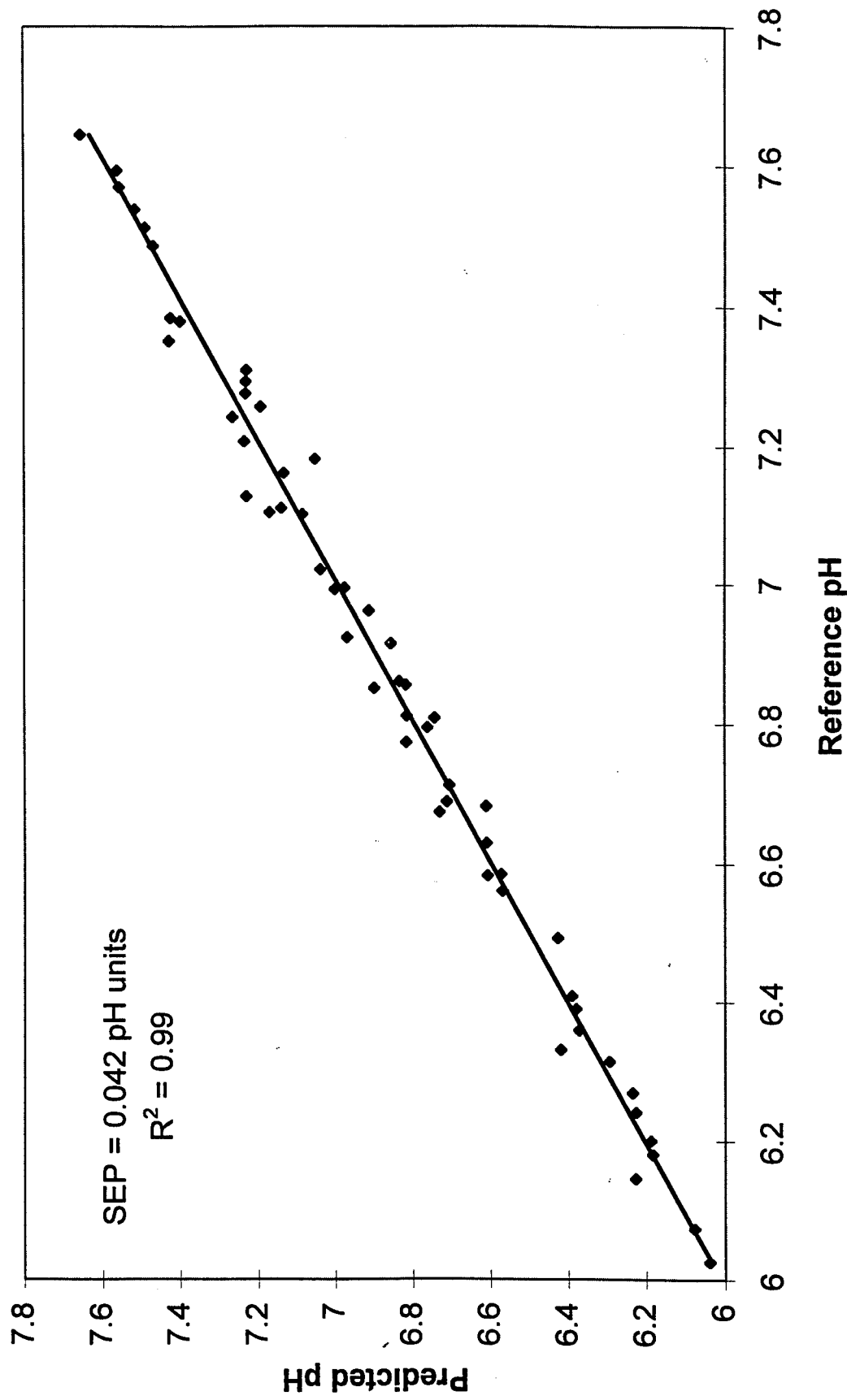


Fig. 17. FT-NIR Si Reflectance Spectra Of Muscle Cell Tissue Phantoms (MCTP2)



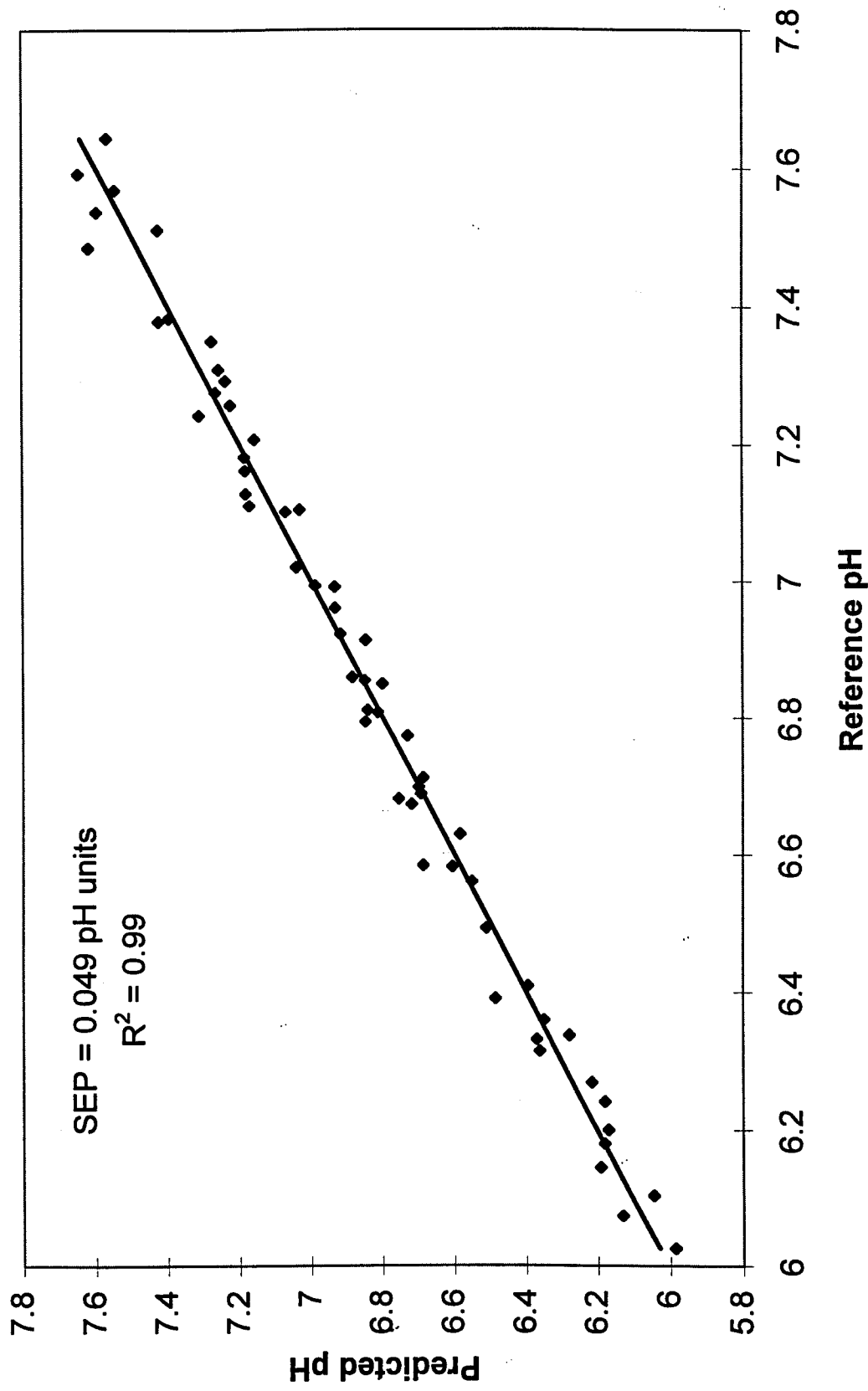
**pH Prediction in Muscle Cell Tissue Phantoms  
Indium Antimonide Detector over 1500 - 1850 nm**

**FIGURE 18**



**pH Prediction in Muscle Cell Tissue Phantoms**  
**Silicon Detector over 580 - 680 nm**

**FIGURE 19**



Received 2/8/2000



**DEPARTMENT OF THE ARMY**  
US ARMY MEDICAL RESEARCH AND MATERIEL COMMAND  
504 SCOTT STREET  
FORT DETRICK, MARYLAND 21702-5012

REPLY TO  
ATTENTION OF:

MCMR-RMI-S (70-1y)

21 Jan 00

MEMORANDUM FOR Administrator, Defense Technical Information Center, ATTN: DTIC-OCA, 8725 John J. Kingman Road, Fort Belvoir, VA 22060-6218

SUBJECT: Request Change in Distribution Statement

1. The U.S. Army Medical Research and Materiel Command has reexamined the need for the limitation assigned to technical reports written for the attached Awards. Request the limited distribution statements for Accession Document Numbers listed be changed to "Approved for public release; distribution unlimited." These reports should be released to the National Technical Information Service.
2. Point of contact for this request is Ms. Virginia Miller at DSN 343-7327 or by email at virginia.miller@det.amedd.army.mil.

FOR THE COMMANDER:

Encl  
as

*Phyllis Rinehart*  
PHYLLIS M. RINEHART  
Deputy Chief of Staff for  
Information Management